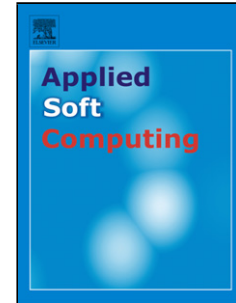


Accepted Manuscript

Title: Type-2 Fuzzy Sets Applied to Multivariable Self-Organizing Fuzzy Logic Controllers for Regulating Anesthesia

Author: Faiyaz Doctor Chih-Hao Syue Yan-Xin Liu
Jiann-Shing Shieh Rahat Iqbal



PII: S1568-4946(15)00647-X
DOI: <http://dx.doi.org/doi:10.1016/j.asoc.2015.10.014>
Reference: ASOC 3252

To appear in: *Applied Soft Computing*

Received date: 22-7-2013
Revised date: 2-2-2015
Accepted date: 8-10-2015

Please cite this article as: F. Doctor, C.-H. Syue, Y.-X. Liu, J.-S. Shieh, R. Iqbal, Type-2 Fuzzy Sets Applied to Multivariable Self-Organizing Fuzzy Logic Controllers for Regulating Anesthesia, *Applied Soft Computing Journal* (2015), <http://dx.doi.org/10.1016/j.asoc.2015.10.014>

This is a PDF file of an unedited manuscript that has been accepted for publication. As a service to our customers we are providing this early version of the manuscript. The manuscript will undergo copyediting, typesetting, and review of the resulting proof before it is published in its final form. Please note that during the production process errors may be discovered which could affect the content, and all legal disclaimers that apply to the journal pertain.

Highlights for Review

Type-2 Self-Organizing Fuzzy Logic Controllers for automatic anesthesia control. • Type-2 SOFLC use type-2 fuzzy sets to handle anesthesia control uncertainties. • Data capturing inter and intra-patient variability used to define type-2 fuzzy sets. • Simulations show effectiveness of type-2 SOFLC in control of anesthetic infusion under noisy and uncertain surgical conditions. • Type-2 SOFLC are able to outperform the existing type-1 SOFLC.

Accepted Manuscript

Type-2 Fuzzy Sets Applied to Multivariable Self-Organizing Fuzzy Logic Controllers for Regulating Anesthesia

Faiyaz Doctor¹ Chih-Hao Syue² Yan-Xin Liu² Jiann-Shing Shieh²
Rahat Iqbal¹

¹*Department of Computing, Coventry University, Coventry, CV1 5FB, United Kingdom*

²*Department of Mechanical Engineering, and Innovation Center for Big Data and Digital Convergence, Yuan Ze University, Chungli, 320, Taiwan, ROC*

Email: faiyaz.doctor@coventry.ac.uk

Abstract--In this paper, novel interval and general type-2 Self-Organizing Fuzzy Logic Controllers (SOFLCs) are proposed for the automatic control of anesthesia during surgical procedures. The type-2 SOFLC is a hierarchical adaptive fuzzy controller able to generate and modify its rule-base in response to the controller's performance. The type-2 SOFLC uses type-2 fuzzy sets derived from real surgical data capturing patient variability in monitored physiological parameters during anesthetic sedation, which are used to define the footprint of uncertainty (FOU) of the type-2 fuzzy sets. Experimental simulations were carried out to evaluate the performance of the type-2 SOFLCs in their ability to control anesthetic delivery rates for maintaining desired physiological set points for anesthesia (muscle relaxation and blood pressure) under signal and patient noise. Results show that the type-2 SOFLCs can perform well and outperform previous type-1 SOFLC and comparative approaches for anesthesia control producing lower performance errors while using better defined rules in regulating anesthesia set points while handling the control uncertainties. The results are further supported by statistical analysis which also show that zSlices general type-2 SOFLCs are able to outperform interval type-2 SOFLC in terms of their steady state performance.

Index terms--anesthesia; hierarchical systems; type-2 fuzzy sets, self-organizing fuzzy logic controller.

1. Introduction

Modern invasive surgical procedures would normally be impossible without the patient being induced into a state of general anesthesia (GA). The essential features of successful GA, displayed by the patient, are a reversible loss of consciousness with a cessation of movement through muscle relaxation, a lack of awareness, unresponsiveness to painful stimuli through analgesia (i.e. pain relief) and an overall lack of recall of the surgical intervention. Inadequate GA may lead to intra-operative awareness with recall (due to anesthetic under dosage) or to prolonged recovery and an increased risk of postoperative complications for the patient (due to over dosage) [1]. The major role performed by a clinical anesthetist is the maintenance of GA over the duration of surgical procedures by the precise and timely delivery of drugs into the patient's body. In order to aid the anesthetist there is a need to design systems to accurately administer and control the delivery of anesthetic in direct response to patients' physiological changes, in order to maintain effective anesthesia during surgery, while providing a means of interpreting these responses. In the last decade several experiments have been performed, where anesthesia was controlled in a closed-loop control system without human interference [2-4]. Although these experiments were relatively successful, there are many sources of complexity and uncertainty related to biomedical control systems that make designing such an automatic controller difficult.

There can be differences in the patient's physiological characteristics such as age, gender and

any pre-operative health conditions which can have an effect on the concentration and duration of anesthetic drug that is required to be administered during surgery [1]. The variability in the physiological effects of drugs on the body (pharmacodynamics) and the drugs metabolism in the body (pharmacokinetics) means that the concentrations of the anesthetic drug required to be infused or inhaled may change. There can be dynamic multi-variable effects in the way the patient responds while undergoing the surgical procedure based on heart rate (ECG), respiration, blood pressure (BP) and muscle relaxation (EMG) as well as brain activity (EEG), which will need to be carefully monitored and controlled by the anesthetist. Finally noise and variability in signals that are sensed and monitored from the human body such with EMG and BP signals can occur due to the effects of high frequency surgical instruments, interference due to changes in cardiac rhythm, sensing barriers such as subcutaneous fat, bodily movements and other external environmental effects. The above mentioned complex multivariable interactions and variations translate into a high degree of non-linearity; complex input output relationships and encountered uncertainties within the control process. These make the task of automating anesthesia control very challenging [5, 6].

Fuzzy logic controllers (FLC) have been credited with being an adequate methodology for designing robust controllers that are able to deliver a satisfactory performance when contending with the uncertainty and imprecision attributed to the real world [7]. FLCs are therefore able to exhibit robustness with regard to noise and variation of system parameters in complex highly non-linear problem domains such as biomedical control systems [8, 9]. There have been a number of recent applications of FLCs for automated drug infusion control as described in [10-12]. Here type-1 FLCs have been used in a closed loop system designed to maintain a targeted effect by adapting the administered amounts of drug based on approximating the outputs of a reference model.

Fuzzy adaptive control schemes in which the FLC parameters are modified have been increasingly applied for regulating the drug delivery process, due to their ability to dynamically configure and learn to control drug infusion/concentration rates based on patient and environmental variability. In [13] a fuzzy rules emulated network (FREN) is described to adaptively control the infusion of Sodium Nitroprusside while maintaining target values for mean arterial pressure (MAP). Here an FLC is initially pre-defined and an on-line adaptation algorithm is used to tune its input and output type-1 membership function parameters during the simulation run. In [14] a fuzzy neural network (FNN) is proposed to automatically manage the hemodynamic variables specifically, MAP and cardiac output (CO), of patients with hypertension and congestive heart failure by simultaneous infusion of cardiac drugs such as vasodilators and inotropic agents. The parameters of the FNN are initialised based on physician expert experience. Over the course of the control simulations a back-propagation learning algorithm adjusts, on-line, the shapes of the type-1 membership functions (MFs) used in the fuzzification layer and fuzzy output layer of the neural network.

Type-2 FLCs that are based on type-2 fuzzy sets have been shown under specific conditions to assist in providing a good solution [15]. This is due to the fact that type-2 fuzzy sets have more design degrees of freedoms, which are able to handle higher orders of possible real world uncertainties and hence potentially contribute to producing more accurate and stable control performances. Previous work by El-Bardini and El-Nagar [16] has developed a direct adaptive interval type-2 FLC for controlling the multivariable anesthesia system to overcome the uncertainty problem introduced by large inter and intra-individual variability of the patient's parameters. This adaptive controller uses predefined rule-bases for each control signal and expert initialized interval type-2 fuzzy sets. The learning mechanism approximates a reference model which models the effects on MAP and muscle relaxation based on the interaction of two

anesthetic agents: Isoflurane and Atracurium used in their regulation to specified set points. This is achieved by a knowledge base modifier which tunes the centers of the output MFs of fired rules in response to deviations from the desired control behaviour. Random initialization of the model parameters was used to simulate the patient variability. More recently in [17] an automatic approach for the regulation of bispectral (BIS) index in the anesthesia process by controlling the concentration target of two drugs, namely, Propofol and Remifentanyl is proposed. The approach constructs a pharmacokinetic and pharmacodynamic patient reference model describing the dynamic reactions to the input drugs which is derived from real clinical data. Three PID controllers are employed, namely linear PID controller, type-1 (T1) fuzzy PID controller and interval type-2 (IT2) fuzzy PID controller, to regulate the BIS index using the nominal patient's model. The number of fuzzy rules and shape of the MFs are initially pre-defined however the PID gains and MF parameters are optimized offline by a Genetic Algorithm subject to a performance index (cost function) which quantifies the performance of the controllers.

One successfully applied approach is the self-organizing fuzzy logic controller (SOFLC) [6] which is composed of a hierarchical control structure consisting of a standard FLC that is adapted using a self-organizing (SO) mechanism proposed by Procyk and Mamdani [6, 18] which acts as a monitor and an evaluator of the controller performance. The SO has the ability to create and modify the rule-base of an FLC to meet the desired response of the controller. This feature provides a qualitative adaptive mechanism which is based on adjusting the control behavior rather than focusing on a parametric tuning and optimization of the fuzzy sets as is the case with the existing approaches for adaptive closed loop drug delivery systems described above. As the rules essentially distribute and individually encapsulate control behavior this approach provides a very flexible adaptive control mechanism that can rapidly adjust the system to a desired behavior. More over the approach can provide the benefit to the anesthetist of being

able to linguistically interpret and analyze the control performance based on adapted rules enabling an understanding of drug delivery behavior over different stages, of specific surgical procedures in response to patient specific physiological and medical conditions.

In the past two decades, there have been several studies on applying SOFLC to biomedical systems, such as muscle relaxation [19, 20], depth of anesthesia [21], and patient analgesia control [22]. Controlling the delivery of anesthesia in operating theaters is possible using the multivariable SOFLC structure due to its ability to approximate flexible nonlinear control models which can be dynamically adapted for regulating desired physiological set points for muscle relaxation and unconsciousness (measured from BP). Simulation studies presented in [6, 23], have shown that the SOFLCs were able to adaptively adjust the multivariate control outputs for the drug concentration and infusion rates however produced high degree of instability and steady state errors in approximating the set points for control of anesthesia, which would not be acceptable in a real system. Part of the reason for this is that these previous applications of SOFLCs are based on using type-1 fuzzy sets, which are unable to handle fully the uncertainties affecting parameter variability associated with biomedical control processes and in particular controlling anesthesia delivery during surgical procedures.

In this paper we propose a type-2 SOFLC which combines the qualitative adaptive control mechanism of a SOFLC with the use of type-2 fuzzy sets to handle the uncertainties affecting parameter variability during the maintenance of anesthetic sedation. Type-2 SOFLC's are based on interval and z-slices based type-2 fuzzy sets [24] which are used for modeling the uncertainties associated with the input / output parameters. We evaluate the performance of the type-2 SOFLCs for the automatic control of anesthesia during single stage surgical procedures in which we use a non-fixed patient model and add signal noise to account for environmental and patient drug interaction uncertainties. We construct the type-2 FOU's using data acquired from

real patients during surgical procedures to approximate realistic patient interaction and signal uncertainties encountered. The FOU's of the type-2 sets therefore aim to capture the possible numerical uncertainties in the physiological parameters during regulation and control of anesthesia. We perform unique simulated experiments in which the type-2 SOFLCs is used for controlling anesthetic drug delivery to maintain physiological set-points for muscle relaxation and BP (used in assessing consciousness) during surgical procedures. We show how our type-2 SOFLCs can deal with the control complexities and uncertainties to produce a good control performance in terms of approximating and maintaining the physiological set-points over steady state control. We compare their performance with type-1 SOFLCs and show the type-2 SOFLCs produce significantly lower performance errors while generating fewer better defined rules in controlling a multi-variable anesthesia system.

The rest of this paper is organized as follows: In Section II, we describe the patient anesthetic model and the derived reference model which we use in our anesthesia control simulations for evaluating controllers' performance. In Section III, the type-2 fuzzy sets and their associated terminologies are introduced. Our type-2 SOFLC's hierarchical control and adaptation mechanism is described in Section IV. In Section V, we present our experiments and results. Finally conclusions and future research directions are presented in Section VI.

2. Patient Anesthetic Model

The major roles performed by a clinical anesthetist are the maintenance of drug-induced muscle relaxation (paralysis), unconsciousness and analgesia [25]. Measuring the patient's level of sensation based on muscle relaxation can be carried by using a Datex Relaxograph to measure evoked electromyogram (EMG) signals. In clinical settings, anesthesiologists have a number of

physiological signs and online measurements including BP, EEG, minimum alveolar concentration and auditory evoked response that can be used selectively for the determination of the patient's anesthetic state [26, 27]. However, anesthesiologists still normally use BP as it is considered as one of the most reliable measures according to clinical standard practices [28, 29] for defining the level of anesthesia that relates to the degree of unconsciousness and depth of anesthesia (DoA) [26]. Currently there is still no validated, routinely used monitor for analgesia [30, 31], and so analgesia is not controlled in this study. Regulation of muscle relaxation percentage is done by EMG responses to the intravenous administration of drugs such as Atracurium, Cis-Atracurium, or Rocurocium. This is normally done by using a syringe pump, like an Ohmeda 9000 or Graseby 3500, via a computer to control the infusion rate [32]. For maintaining DoA, BP (expressed in terms of the systolic pressure over diastolic pressure and measured in millimeters of mercury (mmHg) is used as a guide for administering intravenous drugs such as Propofol or inhalational anaesthetics such as Isoflurane, Desflurane, or Sevoflurane. Typically this is done through using a stepping motor via a computer to control the inhalational gas concentration [33].

Pharmacological modeling is commonly used to describe the metabolism of such drugs [16] which can be used as a basis to create a mathematical model. Pharmacological modeling comprises of two main categories which are: **Pharmacokinetics** (PK), the concentration of drugs in the blood as a function of time and dose schedule interpreted mathematically via compartmental models representing the metabolism of the drug in different parts of the body; **Pharmacodynamics** (PD), the relationship between drug concentration in the blood and its effect [34]. In modern surgery, Atracurium is commonly used for controlling muscle relaxation and Isoflurane or Propofol for controlling anesthesia through BP via their PK-PD compartment models.

2.1 Multivariable Anesthetic Model

The patient model used with our SOFLCs simulations is based on a multivariable anesthetic model combining two pharmacological models the **Atracurium Mathematical Model**: based on the pharmacokinetics and non-linear pharmacodynamics of Atracurium [35] on muscle relaxation (paralysis), and the **Isoflurane Unconsciousness Model**: describing variations of BP (change in MAP) to small changes in concentrations of inhaled Isoflurane

2.1.1 The Atracurium Mathematical Model

According to previous studies [34, 35], the Atracurium pharmacokinetics can be expressed by the following transfer function (1) which describes the pharmacokinetics of the muscle relaxation relating to Atracurium.

$$G_1(s) = \frac{9.94(1+10.64s)}{(1+3.08s)(1+34.42s)} \quad (1)$$

The drug's pharmacodynamics effect can be expressed as the following transfer function [36]:

$$G_{11}(s) = \frac{K_1(1+T_4s)e^{-\tau_1s}}{(1+T_1s)(1+T_2s)(1+T_3s)} \quad (2)$$

where τ_1 is a dead-time (time elapsed until the drug takes effect), K_1 is a coefficient, T_1 , T_2 , T_3 and T_4 are time-constants with the values: $\tau_1 = 1$ min, $K_1 = 1$, $T_1 = 4.81$ min, $T_2 = 34.42$ min, $T_3 = 3.08$ min, $T_4 = 10.64$ min. s refers to the algebraic function derived from applying a Laplace

transform to transform from the time domain to a frequency domain s in order to equate time based effects on the model parameters. In addition, the following Hill equation is used to relate the effect of a specific drug concentration as described in equation (3) [37, 38]:

$$E_{eff} = E_{max} \frac{x_E^\alpha}{x_E^\alpha + (X_E(50))^\alpha} \quad (3)$$

where x_E is the drug concentration, α the power and $X_E(50)$ the drug concentration at 50 percent effect with the following values: $E_{max} = 100$ percent, $X_E(50) = 0.404$ $\mu\text{g/ml}$, $\alpha = 2.98$.

2.1.2 The Isoflurane Unconsciousness Model

Up till now there is still no direct method to measure DoA since the brain activity is too complicated to observe. Clinically, BP is one of the signs that are commonly used to indicate DoA. Based on previous studies in [6, 39], the responses of BP to inhaled Isoflurane concentration is approximately linear when the changes in Isoflurane concentration are less than 5 percent. However, the responses are in general non-linear and time-varying if the changes become large. Therefore, a first-order linear model with a dead-time of 0.42 minutes and a time-constant of 2 minutes is used. In addition, in order to estimate the steady-state gain, it is assumed that a relatively sensitive patient needs 2 percent Isoflurane for a 30 mmHg reduction in mean arterial pressure. Therefore, the model describing variations of BP to inhaled Isoflurane concentration can be written as follows [6]:

$$G_{22}(s) = \frac{\Delta MAP(s)}{U_2(s)} = \frac{K_2 e^{-\tau_2 s}}{1 + T_5 s} \quad (4)$$

where ΔMAP is the change in MAP, τ_2 is a dead-time, T_5 is a time-constant and K_2 is a coefficient with the following values: $\tau_2 = 0.42$ min, $T_5 = 2$ min, $K_2 = -15$ mmHg/percent.

2.1.3 The Interactive Component Model

According to previous studies, the interaction of Atracurium to BP is so small that can be ignore [35, 40]. The interaction of Isoflurane to muscle relaxation is significant and is expressed by the following equation [41]:

$$G_{12}(s) = \frac{K_4 e^{-\tau_4 s}}{(1 + T_6 s)(1 + T_7 s)} \quad (5)$$

where τ_4 is dead time, T_6 and T_7 are time-constants, and K_4 is a coefficient having the values: $\tau_4 = 1$ min, $T_6 = 2.83$ min, $T_7 = 1.25$ min, $K_4 = 0.27$.

2.1.4 The Multivariable Anesthetic Model

Based on the equations (1-5) described in previous sections, the overall multivariable anesthetic model combining muscle relaxation (based on the pharmacokinetics and non-linear pharmacodynamics of Atracurium) and unconsciousness (based on the effects of Isoflurane on BP) can be summarized as the following equation:

$$\begin{bmatrix} Paralysis \\ \Delta MAP \end{bmatrix} = \begin{bmatrix} G_{11}(s) & G_{12}(s) \\ 0 & G_{22}(s) \end{bmatrix} \begin{bmatrix} U_1 \\ U_2 \end{bmatrix} \quad (6)$$

where U_1 is the Atracurium infusion, U_2 is the Isoflurane concentration. In a deployed system U_1 and U_2 would be inputs to an embedded microcontroller that would be used to operate the syringe pump and stepping motor for regulating infusion and inhalation concentration of these drugs respectively.

2.1.5 The Non-Fixed Anesthetic Model with Signal Noise

The traditional fixed patient mathematical models is based on predefined clinical studies [34, 35], and cannot represent the dynamic changes and interactive effects of drugs on a patient during surgical operations (intra-patient uncertainties) and these differences from one person to another (inter-patient uncertainties). In our simulations we experimented with adding values up to 1 percent of white noise to approximate the maximum value of possible parametric uncertainty affecting all parameters in equation (1) to (5) of the multivariable anaesthetic model. By using this non-fixed patient anesthetic model we can account for the possible patient drug interaction uncertainties during our simulations. The strength of physiological signals like muscle relaxation and BP is so small that it is susceptible to interference during measurement. In most cases, the amplitude of noise is up to 20 percent of standard deviation of the signal strength in measuring instruments [42]. We therefore experimented with adding values up to 20 percent white noise to the measured signals (i.e. muscle relaxation and BP value), in order to test the robustness of SOFLCs under real environmental uncertainty. Both the patient interaction and signal noise will enable us to test the features of type-2 SOFLCs, in their ability to handle the encountered

uncertainties. The type-2 SOFLC proposed in this paper uses the non-static anesthetic model as a reference model in a closed loop control of the infusion and concentration rates of Atracurium and Isoflurane to maintain set points for muscle relaxation and BP for regulating DoA as shown in Figure 1. The anesthetic model determines signal values for muscle relaxation and MAP based on the interaction of Atracurium and Isoflurane infusion and concentration rates output by the controller. The model signals with the addition of noise are then compared with reference signals produced from a previous control actuation. The error and integration of error of each signal is calculated to form the closed loop inputs to the controller, as shown in Figure 1. We use integration of error as additional inputs to signal errors in order for the control system to better emulate the gradual pharmacokinetics and pharmacodynamics responses and produce less pronounced oscillatory responses when approaching the desired control set points.

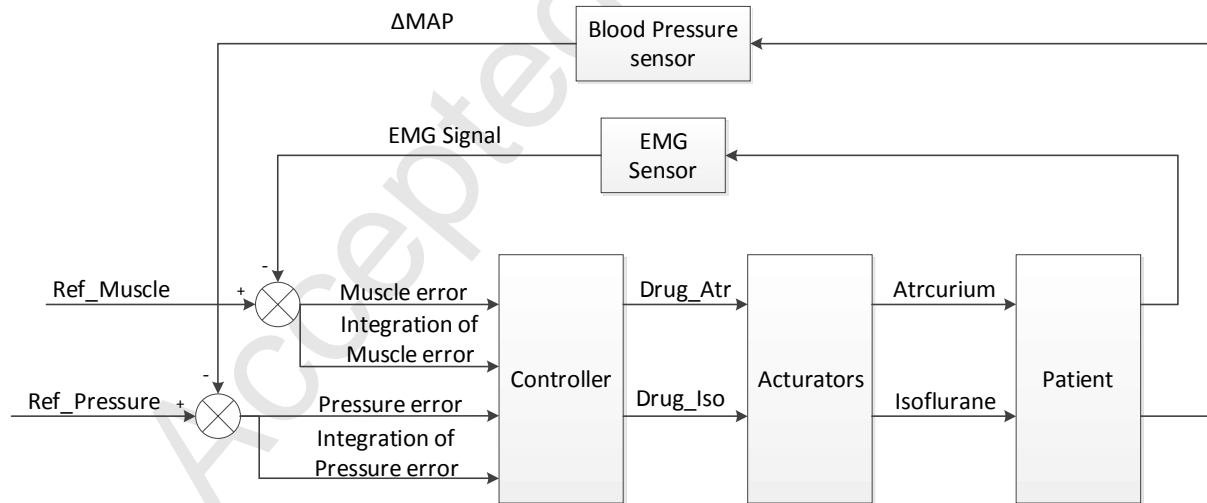


Fig. 1. The block diagram showing the multivariable anesthesia system

3. Type-2 Fuzzy Sets

Type-2 fuzzy sets are characterized by a fuzzy Membership Function (MF), where the membership value (or membership grade) for each element of the set is itself a fuzzy set in $[0, 1]$. This allows us to capture and handle uncertainties about the degree of membership of an element in the fuzzy set. Given an input at p in the case of type-1 fuzzy sets, this will be a crisp singleton membership value where the vertical line intersects the type-1 fuzzy set as shown in Figure 2(a). Note that the figure includes a third dimension which is implicit in the definition of a type-1 fuzzy set [15]. In the case of type-2 fuzzy sets the input at p will no longer have a single crisp value for the MF but instead the MF takes on values wherever the vertical line intersects a bounded area known as the Footprint Of Uncertainty (FOU) of a type-2 fuzzy set, see Figures 2(b), (c) and (d). According to Liang *et al.*[43], a type-2 fuzzy set can be thought of as a large collection of embedded type-1 MFs (forming its FOU), where each type-1 MF also has a weight or amplitude associated with it. These embedded type-1 MFs can potentially partition the input domain into smaller regions which enables a type-2 FLC to realize more complex nonlinear input–output control relationships than a type-1 FLC using the same rule-base [44, 45]. The FOU can be derived from real world domain data [46, 47] to capture the possible control variability of the input / output parameters that will affect the membership degree of their fuzzy sets.

The membership of the type-2 set at p comprises of the primary membership values that intersect the FOU at p . Each primary membership value can have a weight associated with it creating an amplitude distribution projected in the third dimension. This distribution forms what is termed as a secondary MF which provides an additional design degree of freedom for modeling higher level uncertainties associated with the primary membership values. The third dimensional secondary MF can be modeled as either a fixed interval (interval type-2) or as a continuous fuzzy set (General type-2), whose support is in the interval $[0, 1]$ [15], as shown in Figure 2(b) and (c) respectively.

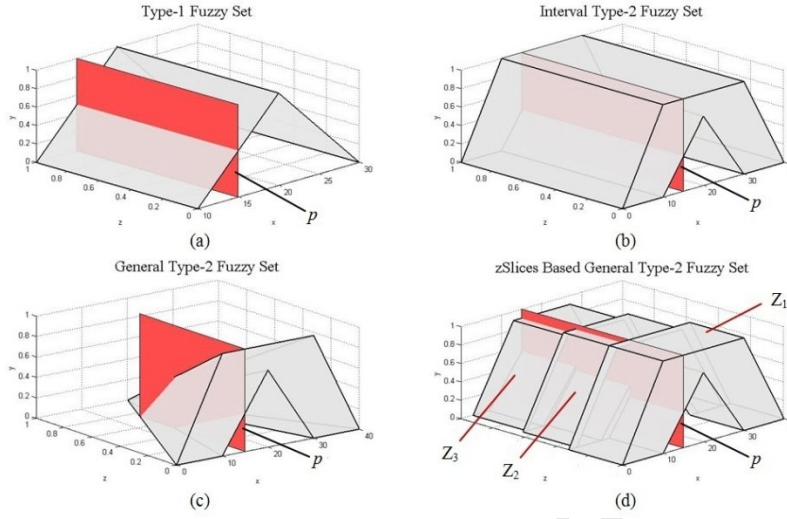


Fig. 2. An example of the three types of fuzzy sets, where the same input p is applied to each fuzzy set showing its vertical intersection and corresponding membership to the set (a) Type-1 fuzzy set (b) Interval type-2 fuzzy set (c) General type-2 fuzzy set (d) zSlices based general type-2 fuzzy set

Formally a general type-2 fuzzy set \tilde{A} is characterized by a type-2 MF $\mu_{\tilde{A}}(p, u)$ [48] where $p \in X$ and $u \in J_p \subseteq [0,1]$, i.e.,

$$\tilde{A} = \{((p, u), \mu_{\tilde{A}}(p, u)) \mid \forall p \in X, \forall u \in J_p \subseteq [0,1]\} \quad (7)$$

in which $\mu_{\tilde{A}}(p, u) \in [0,1]$. \tilde{A} can also be expressed as follows [48]:

$$\tilde{A} = \int_{p \in X} \int_{u \in J_p} \mu_{\tilde{A}}(p, u) / (p, u) J_p \subseteq [0,1] \quad (8)$$

where \coprod denotes union over all admissible x and u . J_p is called the primary membership of p in \tilde{A} . At each value p say $p = p'$, the two-dimensional (2-D) plane, whose axes are u and $\mu_{\tilde{A}}(p, u)$ is called a vertical slice of \tilde{A} [48]. A secondary MF is therefore a vertical slice of \tilde{A} and is $\mu_{\tilde{A}}(p = p', u)$, for $p' \in X$ and $\forall u \in J_{p'} \subseteq [0,1]$ [48], i.e.,

$$\mu_{\tilde{A}}(p = p', u) \equiv \mu_{\tilde{A}}(p') = \int_{u \in J_{p'}} f_{p'}(u) / u \quad J_{p'} \subseteq [0,1] \quad (9)$$

in which $0 \leq f_{p'}(u) \leq 1$. Because $\forall p' \in X$, the prime notation on $\mu_{\tilde{A}}(p')$ can be dropped, and $\mu_{\tilde{A}}(p)$ is referred to as a secondary MF [48], which is a type-1 fuzzy set, also referred to as a secondary set [48]. When $f_p(u) = 1$ is true for $\forall p \in X$, then the secondary MFs are interval sets and we have the case for an interval type-2 MF [48], which characterizes interval type-2 fuzzy sets.

3.1 Interval Type-2 Fuzzy Sets

Interval secondary MFs reflect a uniform uncertainty distribution over the primary memberships of p [48]. Since all the memberships in an interval set are unity, an interval set is represented just by its domain interval, which can be represented by its left and right endpoints as $[l, r]$ [43]. The two endpoints are associated with two type-1 MFs that are referred to as upper MF (UMF) and lower MF (LMF) [49]. The UMF and LMF are bounds for the FOU (\tilde{A}) of an Interval type-2

fuzzy set \tilde{A} [49]. The UMF is associated with the upper bound of FOU (\tilde{A}) and is denoted by $\bar{\mu}_{\tilde{A}}(p), \forall p \in X$. The LMF is associated with the lower bound of FOU (\tilde{A}) and is denoted by $\underline{\mu}_{\tilde{A}}(p), \forall p \in X$ [49]. The interval type-2 fuzzy set \tilde{A} can be represented in terms of its UMF and LMF as follows:

$$\tilde{A} = \int_{p \in X} \left[\int_{u \in [\underline{\mu}_{\tilde{A}}(p), \bar{\mu}_{\tilde{A}}(p)]} 1/u \right] / p \quad (10)$$

Most of the real world applications of type-2 fuzzy sets have used Interval type-2 fuzzy sets [50]. This is due to the high complexity and associated computational requirements involved in the design of general type-2 fuzzy sets. Interval type-2 sets however have a limited ability to represent the secondary membership values $0 \leq f_p(u) \leq 1$ over a vertical slice of \tilde{A} , which are associated with a varied uncertainty distribution in the third dimension. zSlices based general type-2 fuzzy sets as proposed in [24] provides a framework for extending the capabilities of interval type-2 sets to model the unequal uncertainty distribution in the third dimension. This should result in the potential for a superior control performance in comparison to type-1 and interval type-2 based fuzzy systems.

3.2 zSlices Based General Type-2 Fuzzy Sets

The third dimension (z) of a general type-2 fuzzy set can be sliced into a finite number of interval type-2 fuzzy sets (z_i) to form a zSlices based general type-2 fuzzy set as shown in Figure 3 (d).

Each zSlice \tilde{Z}_i is an interval type-2 fuzzy set with a specific height or level z_i that represents the secondary membership or amplitude associated with all the primary memberships over its FOU. As such, the interval type-2 fuzzy set \tilde{Z}_i would have a membership grade $\mu_{\tilde{Z}_i}(p, u)$ in the third dimension that is equal to $0 \leq z_i \leq 1$ [24]. The zSlice \tilde{Z}_i can therefore be written as follows:

$$\tilde{Z}_i = \int_{p \in X} \int_{u \in J_{i_p}} z_i / (p, u_i) \quad (11)$$

where at each p value, zSlicing creates an interval set with height z_i and domain J_{i_p} , which ranges from $\bar{\mu}_{\tilde{A}}(p)_i$ to $\underline{\mu}_{\tilde{A}}(p)_i$, where $1 \leq i \leq I$ and I is the number of zSlices (excluding \tilde{Z}_0 and $z_i = i/I$ [24]. Figure 3 shows zSlices-based type-2 fuzzy set with three zSlices where $\bar{\mu}_{\tilde{A}}(p)_i$ and $\underline{\mu}_{\tilde{A}}(p)_i$ are designated as r_i and l_i respectively, for each slice along a vertical intersection of the set at point p . Hence equation (11) can be written as follows:

$$\tilde{Z}_i = \int_{p \in X} \int_{u \in [\bar{\mu}_{\tilde{A}}(p)_i, \underline{\mu}_{\tilde{A}}(p)_i]} z_i / (p, u_i) \quad (12)$$

and a zSlice \tilde{Z}_i can also be expressed as:

$$\tilde{Z}_i = \{((p, u_i), z_i) \mid \forall p \in X, \forall u_i \in [l_i, r_i]\} \quad (13)$$

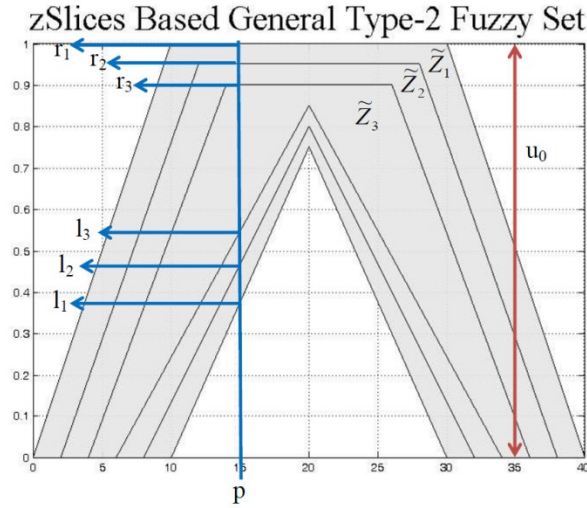


Fig. 3. zSlices-based type-2 fuzzy set with three zSlices where $\bar{\mu}_{\tilde{z}}(p)_i$ and $\underline{\mu}_{\tilde{z}}(p)_i$ memberships (designated as r_i and l_i respectively) are shown for each slice along a vertical intersection of the set at point p

The zSlices are arranged to represent a convex piecewise secondary MF where higher Z levels represent interval type-2 fuzzy sets with more certain narrower FOUs than lower Z level interval type-2 FOUs as shown in Figures 3. Hence depending on the size and shape of the FOUs of each z slice, p would intersect one or more Z levels with corresponding secondary memberships over the union of all intersecting FOUs at z_i .

4. Type-2 SOFLC

Our proposed type-2 SOFLCs for anesthesia control have a closed loop hierarchical adaptation and control structure which has the ability to generate and modify the rule-base making the controller adaptive to dynamic changes in the controlled system. The hierarchical structure consists of two levels comprising of the type-2 FLC and the components of the SO mechanism as

shown in Figure 4 and described in the sections below.

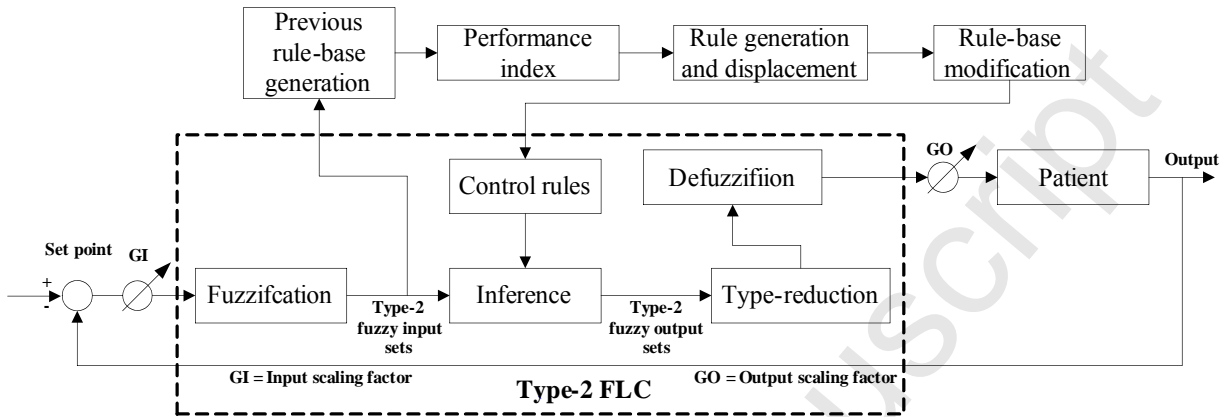


Fig. 4. Type-2 SOFLC control structure with type-2 FLC and SO components

4.1 Type-2 Fuzzy Logic Controller

The first level is a type-2 fuzzy controller which consists of a fuzzifier, inference engine, rule-base, type-reducer, and defuzzifier [43] see Figure 4. The input signal from the patient anaesthetic model to the controller is taken at each sampling instant in the form four inputs. These are the error of muscle relaxation (M_e), integration error of muscle relaxation (M_{e_i}), error of BP (B_e) and integration error of BP (B_{e_i}) based on the set points to be maintained for DOA control. As mentioned the integration of the error is considered as an additional input to the system in order to effect the reduction of the steady state error in approaching the desired control set points. In our previous work we have proposed a method for decomposing a multivariable SO fuzzy logic structure into smaller 2-input/ 1-output control units [6]. This has the advantages of providing a more interpretable and modular component based representation of the system and generated rule-bases, as well as allowing flexible and efficient parallel computational

implementations [51]. In the decomposed 2-input/1-output system used in our simulations, the fuzzy rules can be represented as:

$$\text{IF } \mathbf{x} \text{ is } \tilde{F} \text{ and } \mathbf{y} \text{ is } \tilde{F}, \text{ THEN } \mathbf{z} \text{ is } \tilde{G} \quad (14)$$

where \mathbf{x} and \mathbf{y} are inputs, \tilde{F} is input fuzzy set, \mathbf{z} is output and \tilde{G} is output fuzzy set. In our simulations we evaluate the performance of both four input and two input SOFLCs where in the latter case the input parameters M_e_i and B_e_i are not included. Each input signal is mapped to a corresponding discrete level by using the error and integration error scaling factors respectively.

The type-2 FLC maps control inputs to either interval or zSlices based type-2 input fuzzy sets which are based on singleton fuzzification. The input type-2 fuzzy sets activate rules in the rule-base. The inference engine combines the fired rules by employing type-2 intersection and union operations based on minimum t-norm and maximum t-conorm respectively [43]. This gives a mapping from input type-2 fuzzy sets to output type-2 fuzzy sets (which can also be either interval or zSlices based type-2 output fuzzy sets). The type-2 fuzzy outputs of the inference engine are then processed using standard interval type-2 type-reduction and defuzzification methods. The type-reducer combines the output type-2 fuzzy sets to form a type-1 fuzzy set known as the type reduced set [52]. The type-reduction method used here is the Enhanced Iterative Algorithm with Stop Condition (EIASC) method [53] which has been shown to be more computationally efficient for real world control applications over the well-known Kamik Mendel (KM) iterative procedure [49, 52]. The defuzzifier can then defuzzify the type-reduced type-1 fuzzy outputs to produce the crisp control outputs, where we use the standard centroid type reducer [54]. These control operation are based on using general type-2 fuzzy sets. In the case of z-slices based general type-2 fuzzy sets the interval type-2 control operations previously

described are computed independently on the input and output interval type-2 fuzzy sets for each level z_i . A centre of sets type-reducer is then used to combine all the type reduced sets for each zlevel z_i to create an overall type reduced set [24]. The centroid defuzzifier is finally applied to obtain a final crisp output value as described in [24].

There are two output control signals corresponding the to change of Atracurium infusion rate (d_Atra_inf) and the change of Isoflurane concentration (d_Iso_conc) which are based on the integration of these output values in order to facilitate real-time adjustment of anesthetic dosage. The crisp outputs are converted back to real values using the output scaling factors and sent to the patient anaesthetic model. The model responses are then fed back to the type-2 SOFLC and compared with the set points to calculate the error and integration error of the input control signals.

4.2 Generation of Type-2 Fuzzy Sets

The type-2 SOFLCs which extend on the type-1 SOFLCs use input and output scaling factors to map the real valued parameters to a set of discrete levels for scaled inputs and outputs used in the system [6]. The discrete levels for the scaled control inputs are divided into seven levels represented by equidistant shoulder and triangular type-1 fuzzy sets: negative big (NB), negative medium (NM), negative small (NS), zero (ZE), positive small (PS), positive medium (PM), and positive big (PB). Figure 5(a) shows the input type-1 fuzzy sets for M_e . The discrete levels for the scaled control outputs are divided into four levels also represented by equidistant shoulder and triangular type-1 fuzzy sets: zero (ZE), positive small (PS), positive medium (PM) and positive big (PB). Both scaled input and output type-1 fuzzy sets have an overlap 25 percent of

the total area of each triangular MF. Interval and zSlices based type-2 FOUs are created from monitored physiological parameters of real anesthetized patients where we use the zSlices based type-2 FOUs to capture the intra and inter patient parameter variability. The generated FOUs will model realistic data derived numerical uncertainties affecting the input and outputs. We can then evaluate the SOFLC's ability to handle different proportions of white noise added to the input signals and non-static reference model parameters for approximating these numerical uncertainties during the surgical simulations. The following section describes the heuristic approach used for generating interval and zSlices based FOUs from the patient data.

4.2.1 Heuristic Approach for Calculating Interval and zSlices Based FOUs from Patient Data

The FOUs of the patient derived type-2 fuzzy sets are generated using data acquired from monitoring physiological parameters of real anesthetized patients, in order to account for the uncertain parameter variability during DoA control. Average percentage of muscle relaxation avg_{mr} and standard deviations (\pm) $stdv_{mr}$ and the average BP avg_{bp} and standard deviations (\pm) $stdv_{bp}$ were collected from 15 anesthetized patients while undergoing ear, nose, and throat (ENT) surgical procedures, as shown in Table 1 [55]. The (\pm) $stdv_{mr}$ and (\pm) $stdv_{bp}$ values for a given patient represent the intra patient variability attributed to noise and the PK and PD effects of anesthetic on the patient's body over the surgery duration. Table 1 also contains the mean average and standard deviation values for muscle relaxation and BP which we will designate as $avg_{mr}^{(mean)}$ $stdv_{mr}^{(mean)}$ and $avg_{bp}^{(mean)}$ $stdv_{bp}^{(mean)}$ respectively.

We used the following heuristic process to generate the interval and zSlices based general type-2 fuzzy sets for the type-2 SOFLC input parameters. A coefficient of variation percentage

for muscle relaxation: cv_{mr} and BP: cv_{bp} is initially calculated for each patient (see table 1), as follows:

$$cv_{\delta}^{(t)} = \frac{stdv_{\delta}^{(t)}}{avg_{\delta}^{(t)}} \times 100 \quad (15)$$

where $1 \leq t \leq T$, T is the number of patients and $\delta = mr$ or bp . The calculated cv values are based on 100 percent muscle relaxation and a BP of 100 mmHg. The operating physiological set points for anesthesia used in our simulations are 80 percent muscle relaxation and 110 mmHg (systolic) BP, which we will designate as stp_{mr} and stp_{bp} respectively. The cv values were then scaled to these set points to give the following scaled cv values $cv\Delta_{bp}^{(t)}$ and $cv\Delta_{mr}^{(t)}$ that were calculated as follows:

$$cv\Delta_{\delta}^{(t)} = \frac{cv_{\delta}^{(t)}}{100} \times stp_{\delta} \quad (16)$$

Table 1 shows the calculated mean cv values $cv_{\delta}^{(mean)}$ for muscle relaxation and BP based on the 15 patients which were then scaled to reflect anesthesia set points and are given as $cv\Delta_{mr}^{(mean)}$ and $cv\Delta_{bp}^{(mean)}$ respectively.

To construct the interval type-2 set's FOU's a symmetric uncertainty value $\pm uc_{\delta}$ is calculated as follows:

$$\pm uc_{\delta} = \left(\frac{cv \Delta_{\delta}^{(mean)}}{pr_{\delta}} \right) / 2 \quad (17)$$

where pr_{δ} is the parameter range over which the $cv \Delta_{\delta}^{(mean)}$ values are divided to derive the FOU uncertainty ranges. The calculated $\pm uc_{\delta}$ is added to the end points of the type-1 fuzzy sets to form the interval type-2 FOUs. The type-2 fuzzy sets produced are based on shoulder and trapezoidal interval type-2 MFs. We illustrate how the heuristic process was applied to generate the interval type-2 fuzzy sets for the type-2 SOFLC input variable M_e , based on the patient data in table 1, as follows:

$$avg_{mr}^{(mean)} = 89.69, \quad stdv_{mr}^{(mean)} = \pm 10.95$$

$$cv_{mr}^{(mean)} = (10.95/89.69) \times 100 = 12.21,$$

$$cv \Delta_{mr}^{(mean)} = 12.21 \times 0.8 = 9.77$$

$$pr_{mr} = \pm 7 \text{ (scaled parameter range for } M_e \text{)}$$

$$\pm uc_{mr}^{(mean)} = 1 \times ((9.77 / \pm 7) / 2) = 1.39 / 2 = \pm 0.70$$

As shown in the example above the overlap and support of the original type-1 fuzzy sets was also factored into the final $\pm uc_{\delta}^{(mean)}$ value. In the case of the input M_e this was the product of the support (*which was 4*) and overlap (*which was 0.25*) that equated to 1. This was then multiplied by $\pm uc_{mr}^{(mean)}$ to give the same result. The calculated $\pm uc_{\delta}^{(mean)}$ value above was then used to construct symmetric FOUs to form interval type-2 fuzzy sets which are shown in figure 5(b).

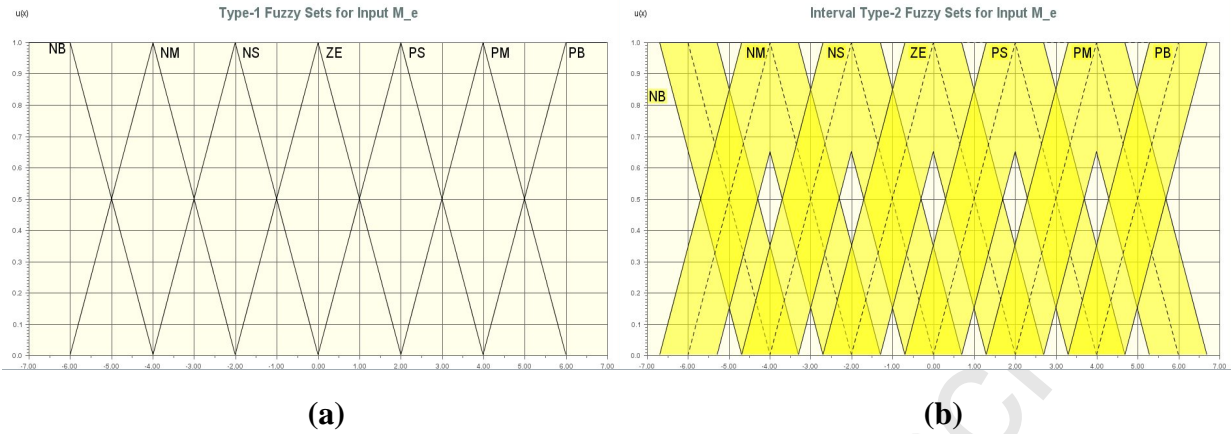


Fig. 5. (a) Type-1 fuzzy sets for input M_e (b) The interval type-2 fuzzy sets (solid lines) and original type-1 fuzzy sets (dashed lines) for input M_e

The cv values $cv_{mr}^{(t)}$ and $cv_{bp}^{(t)}$ for each patient represent inter patient variability attributed to differences in the PK and PD effects of anaesthetic on each patient's body. For constructing the zSlices based general type-2 fuzzy sets, similar inter patient $cv_{\delta}^{(t)}$ values were identified and grouped from the patient data. Five groups of patients were identified, based on a distance measure between their $cv_{\delta}^{(t)}$ values for muscle relaxation and BP respectively. The mean cv values cv_{mr}^i and cv_{bp}^i calculated from each group was used to generate a symmetric interval type-2 FOU_{δ}^i over the endpoints of the original scaled type-1 fuzzy set using the heuristic method previously described, where $1 \leq i \leq 5$. Each FOU_{δ}^i was then assigned to a zSlice with amplitude z_i . The interval FOU's for each group were then arranged together to form a third dimensional piecewise secondary MF of the zSlices based general type-2 fuzzy sets. We illustrate below how the average cv values for muscle relaxation were calculated from each identified group of similar patients based on the patient data in table 1. We then show how the heuristic process was applied to generate the zSlices based general type-2 fuzzy sets for the SOFLC input variable M_e as follows:

$$\text{Patient group 1: } cv_{mr}^1 = 14.11 + 20.88 + 17.60 = 52.59/3 = 17.53$$

$$\pm uc_{mr}^1 (17.53 * 0.8) / 7 = 14.02/7 = 2.0 \text{ (FOU)} = +/- 1.0$$

$$\text{Patient group 2: } cv_{mr}^2 = 13.91 + 13.20 + 12.74 = 39.85/3 = 13.28$$

$$\pm uc_{mr}^2 (13.28 * 0.8) / 7 = 10.62 / 7 = 1.52 \text{ (FOU)} = +/- 0.76$$

$$\text{Patient group 3: } cv_{mr}^3 = 11.71 + 10.95 + 11.84 = 34.5/3 = 11.5$$

$$\pm uc_{mr}^3 (11.5 * 0.8) / 7 = 9.2/7 = 1.31 \text{ (FOU)} = +/- 0.66$$

$$\text{Patient group 4: } cv_{mr}^4 = 10.47 + 10.90 + 10.81 = 32.18/3 = 10.72$$

$$\pm uc_{mr}^4 (10.72 * 0.8)/7 = 8.58/7 = 1.23 \text{ (FOU)} = +/- 0.61$$

$$\text{Patient group 5: } cv_{mr}^5 = 7.79 + 8.39 + 8.10 = 24.28/3 = 8.09$$

$$\pm uc_{mr}^5 (8.09 * 0.8) / 7 = 6.47/7 = 0.92 \text{ (FOU)} = +/- 0.46$$

The calculated $\pm uc_{mr}^i$ values above are then used to construct symmetric FOU's FOU_{mr}^i for each zSlice which are separately shown in figure 6 (a) for linguistic level ZE. The individual FOU's are then combined to form zSlices based general type-2 fuzzy set for linguistic level ZE as shown in figure 6 (b).

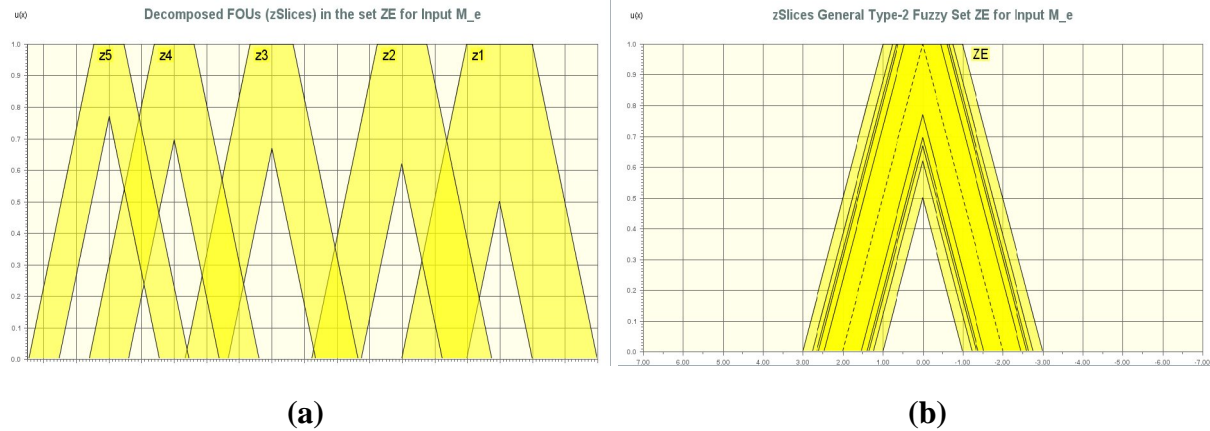


Fig. 6. (a) Decomposed view of the derived FOU_s FOU_{mr}^i for each zSlice (b) zSlices based general type-2 fuzzy set for the linguistic label ZE for input M_e showing the overlapping FOU_s for each slice (solid lines) and the original type-1 fuzzy set (dashed lines)

The type-2 MFs used for the type-2 SOFLC input parameters are constructed using the heuristic method previously described. In contrast a trial and error based approach was used to determine the interval and zSlices based general type-2 MFs used for the type-2 SOFLC output parameters (d_Atra_inf) and (d_Iso_conc). Here the best drug infusion and concentration range to induce patients into anesthesia was determined and then used to calculate the uncertainty ranges for creating the type-2 FOU_s from the existing type-1 fuzzy sets. The design of a more structured approach to generate the output type-2 fuzzy sets will be the scope of future work.

4.3 Self-Organizing Mechanism

The second level of the SOFLC consists of the SO mechanism that is able to tune and modify the control rules to output the desired control responses [6]. The SO mechanism comprises of four functional blocks: the previous rule-base generation, performance index, rule generation and displacement and rule-base modification which feeds into the FLC control rules as shown in Figure 4. The previous rule-base can be generated either from expert experience (i.e., medical doctors) or from learning the input/output relationships based from clinically logged patient data on DoA. During the control process the rules in the previous rule-base generation block will be modified by the SO mechanism. The performance index measures the deviation from the desired response and calculates the appropriate changes that are required in the output of the controller.

The performance index functions act as an evaluation criterion of the controller performance and measures the deviation from the desired trajectory and issues the appropriate correction to the rule(s). It is derived from linguistic conditional statements by means of using standard fuzzy operations and is written in a multi-dimensional look-up table (performance index matrix). The generation and modification of the control rules is achieved by assigning a credit or reward value to the individual rule combinations defined in the look-up table. The credit value is obtained from the performance index defining the desired performance linguistically and is added into a look-up table to generate new rules if these are not found in the previous rule-base. Hence this process will iteratively modify the output of the controller. The type-2 FLC rules are adjusted over the control process to reflect a qualitative “feel” for the patients’ responses to administered drugs and are intended to provide fast convergence around the equilibrium state to achieve a high accuracy and control stability. As the performance functions are only shown in a two-dimensional form, we use our previously described method for decomposing an m-input/n-output SOFLC structure to many 2-input/1-output subsystems whose outputs are then aggregated together as described in [6]. The performance index rules for the 2-input/1-output subsystems can therefore be more easily defined in a more interpretable two-dimensional space [6]. Figure 7 shows our four input two output type-2 SOFLC which has been decomposed into 12 two inputs/one output subsystems. Further details on the design of SOFLC can be found in [56]. The type-2 SOFLC therefore provides adaptive control rules which can effectively model a multivariable non-linear system and dynamically configure themselves to control drug infusion/concentration rates while handling patient and environmental uncertainties.

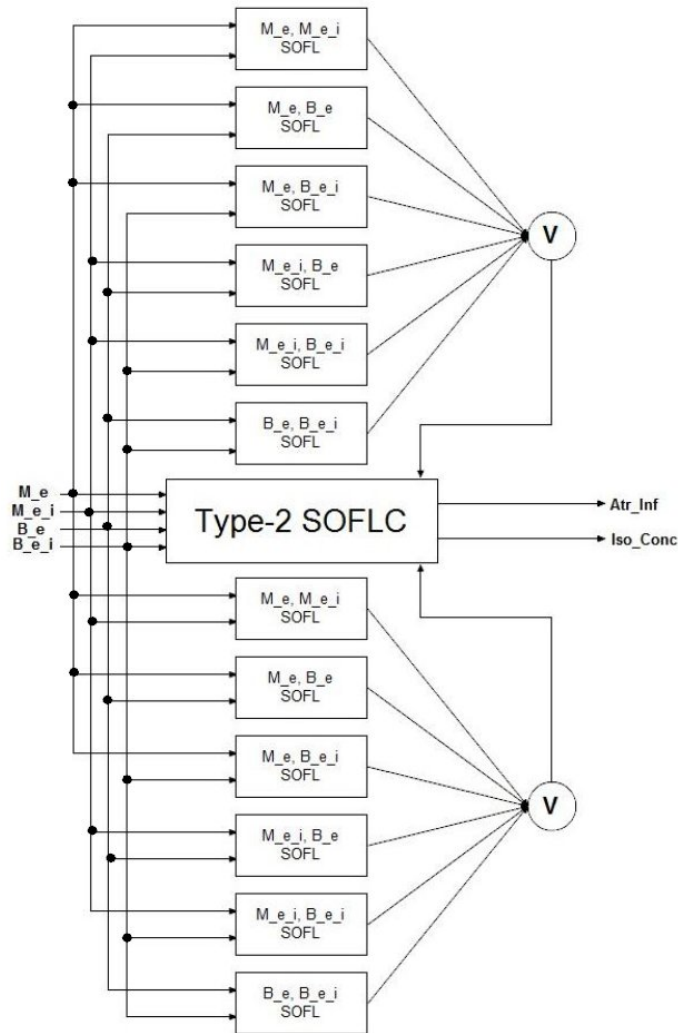


Fig.7. The decomposition of 4-input / 2-output SOFLC structure into 2 input / one output subsystems

5. Experiments and Results

Unique simulations are presented in which we evaluate the interval and zSlices based general type-2 SOFLCs in comparison with the existing type-1 SOFLC. The simulations compared the performance of each controller in their abilities to effectively control the infusion and concentration rates for Atracurium and Isoflurane to regulate set points for muscle relaxation and BP in the face of noisy signals. A non-fixed multivariable anesthetic model of the

Pharmacokinetic and Pharmacodynamics effects of these drugs, that would account for possible uncertain variability in these effects was used as the patient reference model, as described in section 3.

5.1 Experimental Setup

From point view of clinical measurements, in order to measure muscle relaxation stimulating electrodes for a Datex Relaxograph are placed over the ulnar nerve of the non-infused hand, while sensing electrodes are placed over the hypothenar area. By stimulating the nerve the expected degree of neuromuscular block is determined based on EMG [33]. To measure BP previous studies have used a MP60 critical care patient monitor to measure patients' MAP at one minute intervals [21]. In our simulations Muscle relaxation percentage was normalized over a scale of 0-1 where the initial value of muscle relaxation was set at 0. BP was measured in units of mmHg and was initialized to 120 mmHg. In our previous work the initial default values of EMG set points used were between 10 and 20 percent of the baseline based on different surgical needs for adequate muscle relaxation [32]. Hence we used an EMG set point at 20 percent of the baseline for our simulation of muscle relaxation which corresponded to a normalized output value of 0.8. During anesthesia it is normal practice to reduce MAP by 10~15 percent in comparison with conscious states of patients. Hence, we used a set point of 110 mmHg for BP in this study. Each controller was evaluated on its ability to maintain the desired set points for muscle relaxation and BP that are considered acceptable for DoA during surgery as previously discussed in [6].

In modern surgical procedures it is usual practice to administer an initial bolus of anesthetic to

patients in order to raise its concentration in blood to an effective level in order to reach rapid anesthesia and unconsciousness [57]. This is often administered intravenously, by intramuscular, intrathecal or subcutaneous injection. Rapid anesthesia can help to initially stabilize the patient prior to surgery, after which the anesthetist can control the drug delivery rates to regulate DoA. In our simulations, an initial bolus is modeled based on Atracurium, which is administered to patients to reach the saturation of muscle relaxation (near to 1 normalized scale of muscle relaxation), where the range of muscle relaxation is between 0 to 1 normalized units. The amount of Atracurium injected to the patients is about 5 normalized units for the first 5 minutes. During 5 to 15 minutes, the muscle relaxation which reaches almost saturation settles down to be near to the desired set point for 10 minutes. Because the Atracurium effects muscle relaxation and has virtually no effect on consciousness (i.e., BP), the patient's BP is maintained constant at 120 mmHg for the first 15 minutes via only the effect of Isoflurane. In clinical operations, it is usual to give intravenous administration of Propofol as an initial bolus to quickly bring patient into an unconscious state and then use Isoflurane to maintain the anesthesia level. However In these simulations we do not include a model of the effects of Propofol on BP, which we consider to be a possibility for future work. Following the initial bolus effect, the SOFLC controller is turned on to control multivariable anesthesia system.

For each SOFLC the performance of two different input configurations were tested, specifically a 2-input 2-output SOFLC and a 4-input 2-output SOFLC which included the integration of error inputs B_{e_i} and M_{e_i} in addition to the two existing inputs B_e and M_e as described in [6]. We will use the following shortened naming conventions to reference the different SOFLCs being evaluated: $##-T1-SOFLC$ for the type-1 SOFLC, $##-IT2-SOFLC$ for the interval type-2 SOFLC and $##-GT2-SOFLC$ for the zSlices based general type-2 SOFLC, where $##$ represent to number of inputs and outputs of the SOFLC respectively. The simulations were

run using MATLAB on a desktop PC with an Intel(R) Pentium(R) Dual CPU E2180, running MS Windows 7. Each simulation was run for 15,000 intervals where 100 intervals represent 1 minute of time. Hence the total time for each simulation was 150 minutes which is a realistic time frame for single stage procedures such as ear, nose, and throat (ENT) operation.

5.2 Type-1 and Type-2 SOFLCs Simulations and Evaluation

The strength of physiological signals like muscle relaxation and BP is very small and susceptible to interference when measuring. Examples of this can be due to the use of high frequency surgical instruments (e.g., electrosurgical unit), heart beat irregularity or subcutaneous fat. In most cases, the amplitude of noise is up to 20 percent standard deviation of the signal strength in measuring instruments [42]. Consequently, simulations based on both noise free and a noise added environments were performed. In the simulations on a noise added environment, 5, 10, 15, and 20 percent of signal noise was added to the measured signals (i.e. muscle relaxation and BP values), in order to test the robustness of the different SOFLCs (T1, IT2 and GT2) under real environmental uncertainty based on using a fixed (noise free) patient model. As previously mentioned we also experimented with adding values of up to 1 percent of white noise to approximate the maximum value of possible parametric uncertainty affecting all parameters in equation (1) to (5) of the multivariable anesthetic model. Hence we tested each SOFLC's simulation performance in relation to the effects of using a non-fixed patient model with added white noise values of 0.25, 0.50, 0.75 and 1 percent, while keeping the signal noise at zero. Finally a performance evaluation of each SOFLC was carried out by simultaneously introducing the maximum possible single noise of 20 percent standard deviation of the signal strength to the

measured signals and the maximum possible added white noise of 1 percent to the non-fixed patient model. Since the added white noise affects the physiological signal measurements in a random way, we repeated each simulation 10 times to account for these effects in our analysis.

The performance of each SOFLC controller on the surgical simulation was evaluated against the following performance measures for which the mean and standard deviation values were obtained over the 10 simulation runs are presented in Tables 2 and 3: Steady State Errors for muscle relaxation (SSE_M) and BP (SSE_P) was used to evaluate the performance of the controller in its ability to approximate and maintain the desired set points over the duration of the simulation. This was based on the absolute error calculated from the different between the actual and desired set point values to be maintained, based on the average values over the last 50 minutes of simulation). The Overshoot Error for muscle relaxation (OS_M) was used to define the percentage error between maximum muscle relaxation percentage value and average of steady state values produced during the simulation. The Undershoot Error for BP (US_P) was defined as the percentage error between minimum BP value and average of steady state values obtained over the duration of simulation. There were two additional performance measures also used as follows: The Rising Time error for muscle relaxation (RT_M), that was based on the time taken to rise the muscle relaxation percentage from 10 percent to 90 percent of the steady state value and the Decreasing Time error for BP (DT_P) that was defined as the time taken to decrease BP from 10 percent to 90 percent of the steady state value. As a control system, an SOFLC that produce less RT_M or DT_M has a better performance. Although the data results of each of the repeated simulations were different due to the addition of noise, the simulated drug induced muscle relaxation and BP values of each SOFLC converged to similar values among the 10 repeated simulations. Therefore, we chose typical output cases produced by each controller corresponding to the added amounts of signal and model noise to construct our simulation plots

for analysis.

Figures 8, 9, 10 and 11 show the simulation results on noise free environment, and Table 2 shows the detail data in terms of SSE, RT_M, DT_P, OS_M and US_P. The simulation results in Figures 8(a), 9(a), 10(a) and 11(a) compare the equivalent two input type-1, interval type-2 and general type-2 SOFLCs initiated with bolus. Figures 8(a) and 9(a) show that the 22-T1-SOFLC was unable to reach the desired set points for both muscle relaxation and BP over the entire duration of the surgical simulation. In comparison the 22-IT2-SOFLC initially resulted in a marginally higher RT_M in regulating muscle relaxation. However the controller was able to quickly stabilize and reach the desired set point with a considerably reduced SSE_M, as shown in Figure 8(a). The 22-IT2-SOFLC was also successful in regulating BP at its desired set point. There was an initially higher DT_P than the 22-T1-SOFLC though the US_P and SSE_P were considerably reduced as compared with the T1-SOFLC as shown in Figure 9(a). The simulation results for the 22-GT2-SOFLC showed that the controller initially produced a higher DT_P in reaching the BP set point compared to the equivalent type-1 and interval type-2 systems and higher US_P in stabilizing compared to the T1-SOFLC. The controller was however able to outperform both the 22-T1-SOFLC and 22-IT2-SOFLC in terms of a reduced SSE_P and SSE_M as shown in Figures 8(a) and 9(a). The simulation results in Figures 8(b), 9(b), 10(b) and 11(b) compare the equivalent four input type-1, interval type-2 and general type-2 SOFLCs initiated with bolus. The 42-IT2-SOFLC was shown to perform better in terms of reduced SSE_M and US_P errors than the 42-T1-SOFLC which was unable to reach the desired muscle relaxation set point over the duration of the simulation, as shown in Figure 8(b). The SSE_P and RT_M for the 42-IT2-SOFLC were however higher in comparison to the type-1 system. The 42-GT2-SOFLC initially produced a higher US_P compared to the 42-T1-SOFLC and 42-IT2-SOFLCs, however achieved a lower SSE_M than both the 42-IT2-SOFLC and 42-T1-SOFLC. In

the comparisons described above we did not compare OS_M values as we found that for the cases that used initial bolus, the OS_M values actually only depend on the steady state value of each SOFLC because the maximum value of muscle relaxation occurs at initial bolus stage as Figure 8 shows. Consequently, the comparison of OS_M is meaningless.

Figure 12 shows the simulation results of 4-input 2-output SOFLCs (*initialized with bolus*) under 20 percent signal noise and 1 percent model noise, while Table 3 shows corresponding data in terms of SSE, RT_M, DT_P, OS_M and US_P. Figure 12(a) shows that the three SOFLCs produce similar performance for controlling muscle relaxation. However, from Figure 12(c) we can find the Atracurium infusion of 42-T1-SOFLC has more fluctuation than 42-IT2-SOFLC and 42-GT2-SOFLC. Therefore, we can conclude that 42-IT2-SOFLC and 42-GT2-SOFLC have better control stability in terms of muscle relaxation control. As for BP, from Figure 12(b), we can see 42-T1-SOFLC has an offset and also fluctuates wildly, whereas 42-IT2-SOFLC and 42-GT2-SOFLC are able to keep steady at the set point. The wild fluctuation of isoflurane curve produced by 42-T1-SOFLC in Figure 12(d) also supports the phenomenon in Figure 12(b).

In order to make a more precise performance comparison of the SOFLCs, the Kruskal–Wallis and Wilcoxon signed-rank tests were applied to analyze their SSE [58, 59]. Both the two tests are non-parametric tests. The former can test the equivalence of two or more groups of samples, while the latter is used for the comparison of two paired samples. Firstly, we use the Kruskal–Wallis test to find whether there existed a significant difference among the different 4-input 2-output SOFLCs (*initialized with bolus*). As we evaluate a total of 9 different noise strengths and 2 SSE data types (*namely for muscle relaxation and BP*), there are 18 cases in total. The result of Kruskal–Wallis test shows that all the 18 cases have significant difference. Hence, we applied the one-tailed Wilcoxon signed-rank tests whose significance level α was 0.05 to evaluate the performance of the three SOFLCs. Three groups of pairwise comparisons were set, 42-T1-

SOFLC and 42-IT2-SOFLC, 42-T1-SOFLC and 42-GT2-SOFLC, and 42-IT2-SOFLC and 42-GT2-SOFLC. The result of the three comparisons are shown in Table 3 where the cases rejecting the tested performance hypotheses for each pairwise comparison are marked with superscript ^a, ^b and ^c respectively. The result of comparison between 42-T1-SOFLC and 42-IT2-SOFLC shows that only 1 of the 18 tests reject the hypothesis that 42-T1-SOFLC and 42-IT2-SOFLC are different. Note that in terms of SSE_M, of the four simulations under zero signal noise, the 42-T1-SOFLC produces a lower mean value of SSE_M than 42-IT2-SOFLC, with the results being the opposite in other cases. Therefore, we can conclude that in 13 of the 18 cases, 42-IT2-SOFLC performs better. Of the remaining 5 cases shown in 4 cases the 42-T1-SOFLC performs better, and in 1 case they are comparable. Similarly, 42-GT2-SOFLC performs better than 42-T1-SOFLC in 13 of the 18 cases, worse in 2 of the 18 cases, and comparable to 42-T1-SOFLC in 3 cases. The results of comparison between 42-IT2-SOFLC and 42-GT2-SOFLC are that 42-GT2-SOFLC performs better in 14 cases and are comparable in the remaining 4 cases. Finally 6 groups of overall pairwise comparisons (i.e., 42-T1-SOFLC versus 42-IT2-SOFLC, 42-T1-SOFLC versus 42-GT2-SOFLC, and 42-IT2-SOFLC versus 42-GT2-SOFLC in terms of SSE_M, and the same three pairs in terms of SSE_P) combining the 18 cases applying Wilcoxon signed-rank tests were conducted. The results show that 42-T1-SOFLC is not significantly different from 42-IT2-SOFLC and 42-GT2-SOFLC in terms of SSE_M, but significant differences exist in the other 4 groups (i.e., 42-IT2-SOFLC versus 42-GT2-SOFLC in terms of SSE_M and the other three tests in terms of SSE_P). Based on both of the overall mean of SSE_M and the overall mean of SSE_P, the 42-GT2-SOFLC produces the lowest value, the 42-T1-SOFLC produces the largest value and the 42-IT2-SOFLC produces a medium value between those of the other two controllers. Thus it is clear to see that the 42-GT2-SOFLC performs best and the 42-T1-SOFLC performs the worst in terms of SSE_P. For the SSE_M, the reason why 42-T1-

SOFLC is not significantly different from 42-IT2-SOFLC and 42-GT2-SOFLC is that the 42-T1-SOFLC performs well for the cases without signal noise but worse than 42-IT2-SOFLC and 42-GT2-SOFLC for the cases with signal noise as we have previously described. However, in a practical scenario signal noise is unavoidable, so we can still conclude that 42-GT2-SOFLC performs best and 42-T1-SOFLC performs worst in terms of SSE_M.

Statistical comparison of RT_M, DT_P, OS_M and US_P between each SOFLC were also conducted. Firstly, the Kruskal–Wallis test was applied to determine if there existed significant difference among the three SOFLCs, whose results are shown in Table 3 where the cases rejecting this hypothesis are marked with the superscript ^d. We then performed the Wilcoxon signed-rank test to rank the three SOFLCs for the cases where significant differences occurred. In regards to the comparison of RT_M and DT_P, the RT_M values are comparably similar between all three systems due to the initial bolus effect. The DT_P results show that for all the cases where only model noise was added, the 42-IT2-SOFLC outperformed the 42-T1-SOFLC. However when signal noise was added, the results show there are three cases without significant difference, and three cases where the 42-T1-SOFLC has a lower DT_P than the type-2 SOFLCs (i.e., 42-IT2-SOFLC and 42-GT2-SOFLC). The reason for this could be that after signal noise was added, the 42-T1-SOFLC was not able to reach set point as Figure 12 (b) shows. Thus the difference between steady state value and initial value for 42-T1-SOFLC was decreased, which leads to a reduced DT_P. In terms of OS_M, the resulting values do not show any performance differences between the different SOFLCs for the same reason as the result under noise free environment which we illustrated above. The results of US_P are the opposite of those of DT_P. That is, the US_P values of 42-T1-SOFLC are less than those of 42-IT2-SOFLC and 42-GT2-SOFLC for the cases where model noise was added, but the US_P values of 42-T1-SOFLC are larger than those of 42-IT2-SOFLC and 42-GT2-SOFLC for the cases where signal noise was

added. However, despite the difference of each SOFLC, the US_P values of all these cases are all quiet good as they are only around 1 percent.

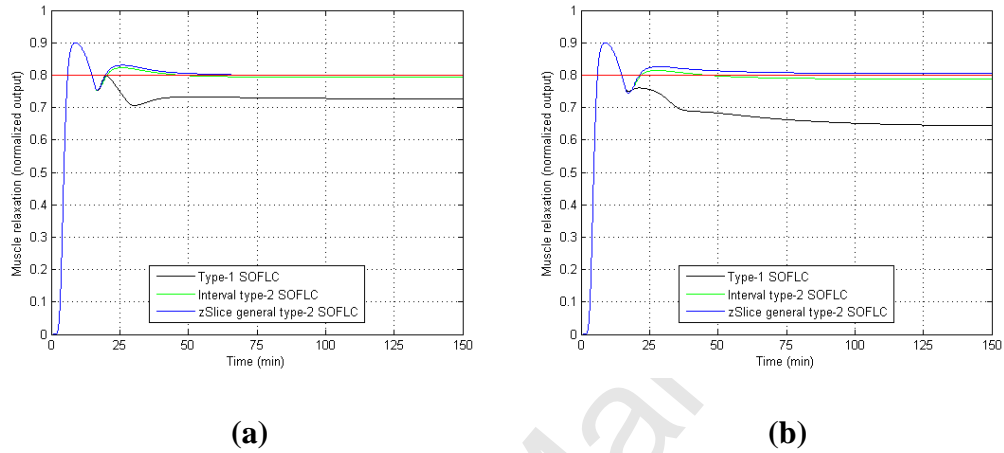


Fig. 8 The simulation result of muscle relaxation on noise free environment using (a) 2 input 2 output SOFLC (b) 4 input 2 output SOFLC

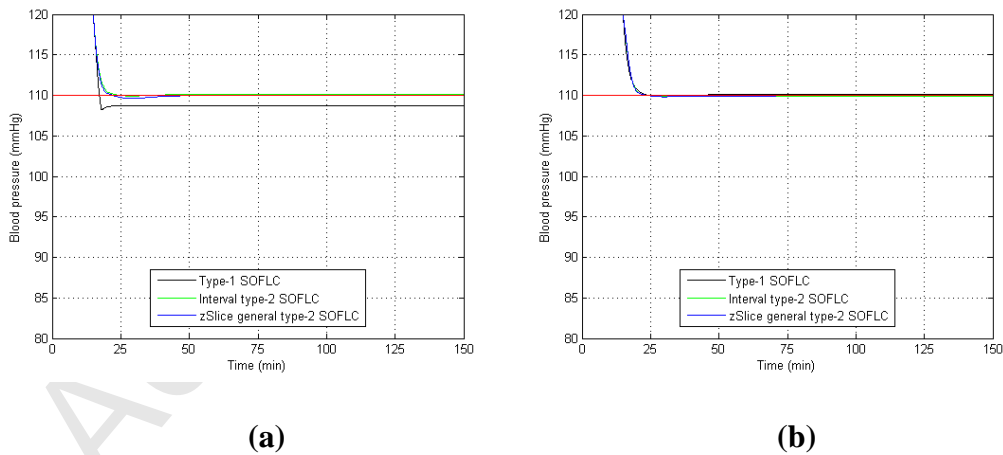
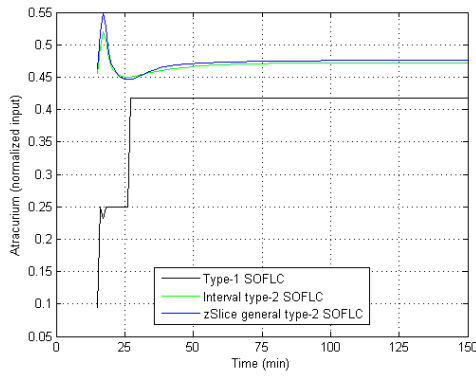
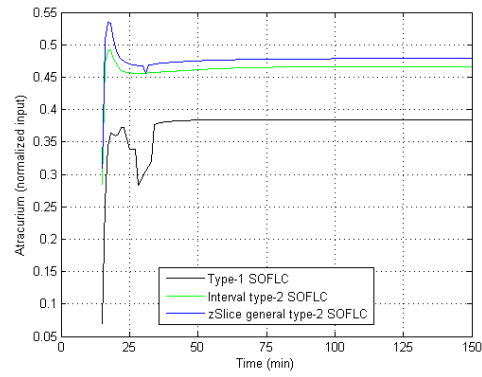


Fig. 9 The simulation result of BP noise on free environment using (a) 2 input 2 output SOFLC (b) 4 input 2 output SOFLC

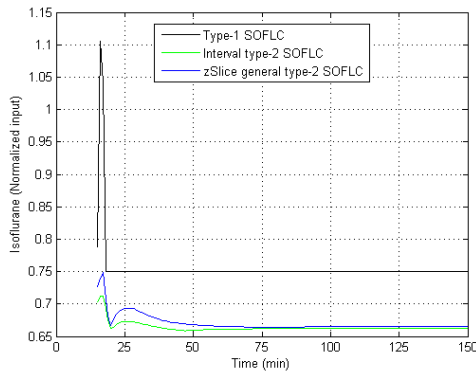


(a)

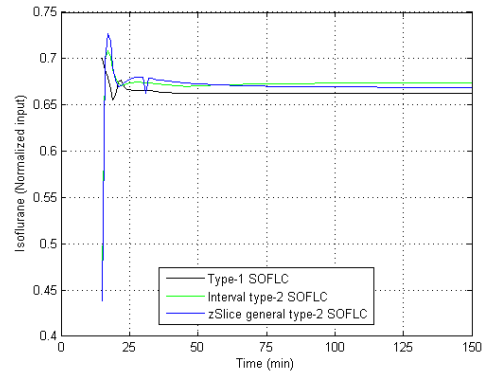


(b)

Fig. 10 The simulation result of Atracurium infusion on noise free environment using (a) 2 input 2 output SOFLC (b) 4 input 2 output SOFLC



(a)



(b)

Fig. 11 The simulation result of Isoflurane concentration on noise free environment using (a) 2 input 2 output SOFLC (b) 4 input 2 output SOFLC

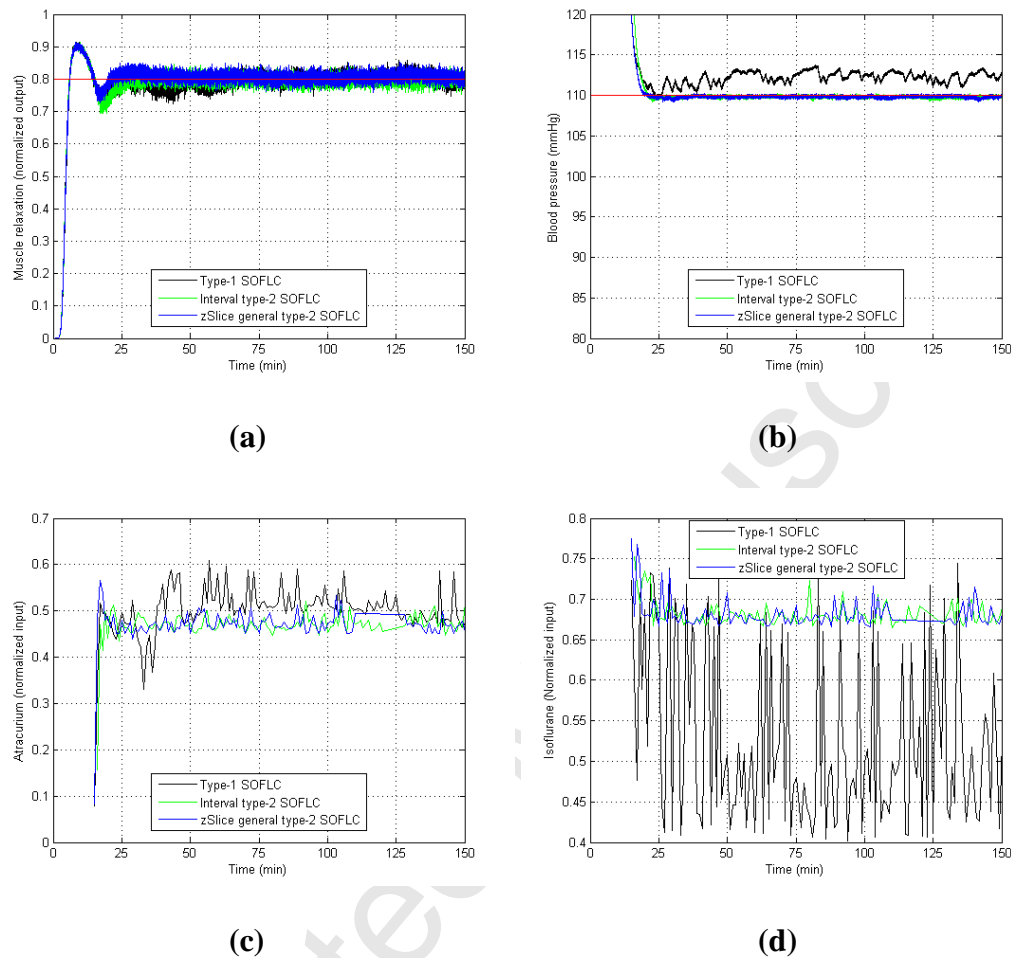


Fig. 12 The simulation result of 4 input 2 output SOFLCs under 20 percent signal noise and 1 percent model noise (a) muscle relaxation (b) BP (c) Atracurium infusion (d) Isoflurane concentration

We also conducted simulations comparing the performance of type-1 and type-2 SOFLCs without the use of an initial bolus under the noise free simulation conditions as described in the experiments above. Although these simulations are not presented here the performance results which are presented in table 2 conclude that the 42-T1-SOFLC was able to reach set points for BP and muscle relaxation although it took too long to reach the desired set point for the latter which is unacceptable for anesthesia control. In comparison both the 42-IT2-SOFLC and 42-GT2-SOFLC were able to produce a better multivariable control performance reaching the

steady state set points for both inputs in just a few minutes. Both these systems however encountered an initially high undershoot error for BP that would have caused a patient's blood pressure to fall dangerously low during the DoA control process. It was therefore necessary to use an initial bolus with the type-2 SOFLCs to allow the system to quickly stabilize and our simulations in figure 8 to 12 shows that this provides a more stable steady state multi variable control performance as compared to the type-1 system.

5.3 Rule-base Analysis of Type-1 and Type-2 SOFLCs

In order to analyze the behavior characteristics of the SOFLCs, we logged the rule firing percentage (calculated as the number of times that a rule was fired divided by total number of inference operations) of each SOFLC running on maximum noise environment (i.e., 20 percent signal noise and 1 percent model noise). The initial rule-base of 4 input 2 output SOFLC is shown in figure 13. Figure 14 and 15 show the firing percentage of the final rule-base for Atracurium and Isoflurane outputs respectively. The x-y planes of figure 14 and 15 correspond to figure 13. The height of each bar shows the output linguistic term of each rule and the color represents the firing percentage in reference to the color bar on the right. Since those rules that were fired less than 1% of the total number of inference operations were mainly fired due to noise, we considered them to be trivial rules and set them to be white. The first column on the left and top row in figure 13 represent the linguistic labels for the error and integration error respectively of each input parameter (muscle relaxation and BP). The intersection of each identical set of these linguistic labels form a block of six cells which represent the output linguistic label corresponding to the six decomposed 2 input combinations (i.e., error of muscle

relaxation and integration error of muscle relaxation, error of muscle relaxation and error of BP, error of muscle relaxation and integration error of BP, integration error of muscle relaxation and error of BP, integration error of muscle relaxation and integration error of BP, error of BP and integration error of BP). Each of the cells in figure 13 therefore represents a decomposed 2 input 1 output rule. By comparing the rule-bases of the different SOFLCs, we can see from the generated and active rules in both Figures 14 and 15, the 42-T1-SOFLC used more rules than 42-IT2-SOFLC and 42-GT2-SOFLC. 42-GT2-SOFLC used the least number of rules and a more noteworthy phenomenon is that the rules used by 42-GT2-SOFLC are concentrated on the middle of the rule table, which indicates stable control around the ZE state. Therefore, we can conclude that 42-T1-SOFLC has to use more rules to handle noise and control uncertainties, whereas 42-IT2-SOFLC and 42-GT2-SOFLC are able to achieve a steadier control behavior with less used rules because their type-2 fuzzy sets can handle more uncertainties than those of 42-T1-SOFLC.

ATR	NB			NM			NS			ZE			PS			PM			PB		
NB	PB	PB	PB				PB	PM	PB				PM	PS	PB				PM	PS	PB
	PB	PB	ZE				PB	PB	ZE				PB	PM	ZE				PB	PM	ZE
NM				PM	PM	PM				PM	PM	PM				PM	PS	PM			
				PM	PM	ZE				PM	PM	ZE				PS	PM	ZE			
NS	PS	PM	PS				PS	PS	PS				ZE	PS	PS				ZE	PS	PS
	PM	PS	ZE				PM	PS	ZE				PS	ZE	ZE				PS	ZE	ZE
ZE				ZE	ZE	ZE				ZE	ZE	ZE				ZE	ZE	ZE			
				ZE	ZE	ZE				ZE	ZE	ZE				ZE	ZE	ZE			
PS	ZE	ZE	ZE				ZE	ZE	ZE				ZE	ZE	ZE				ZE	ZE	ZE
	ZE	ZE	ZE				ZE	ZE	ZE				ZE	ZE	ZE				ZE	ZE	ZE
PM				ZE	ZE	ZE				ZE	ZE	ZE				ZE	ZE	ZE			
				ZE	ZE	ZE				ZE	ZE	ZE				ZE	ZE	ZE			
PB	ZE	ZE	ZE				ZE	ZE	ZE				ZE	ZE	ZE				ZE	ZE	ZE
	ZE	ZE	ZE				ZE	ZE	ZE				ZE	ZE	ZE				ZE	ZE	ZE

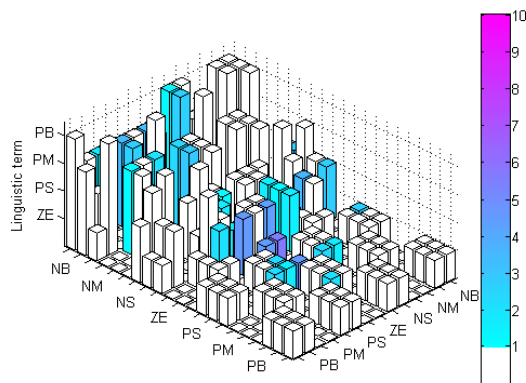
(a)

ISO	NB			NM			NS			ZE			PS			PM			PB		
NB	ZE	PB	ZE				ZE	PS	ZE				PM	ZE	PM				PB	ZE	PB
	ZE	ZE	ZE				ZE	ZE	ZE				PM	PM	ZE				PB	PB	PS
NM				ZE	PM	ZE				ZE	ZE	ZE				PM	ZE	PM			
				ZE	ZE	ZE				ZE	ZE	ZE				PM	PM	PS			
NS	ZE	PM	ZE				ZE	PS	ZE				PS	ZE	PS				PM	ZE	PM
	ZE	ZE	ZE				ZE	ZE	ZE				PS	PS	PS				PM	PM	PM
ZE				ZE	ZE	ZE				ZE	ZE	ZE				PS	ZE	ZE			
				ZE	ZE	ZE				ZE	ZE	ZE				PS	PS	PM			
PS	ZE	ZE	ZE				ZE	ZE	ZE				PS	ZE	ZE				PS	ZE	ZE
	ZE	ZE	ZE				ZE	ZE	PS				PS	PS	PS				PS	PS	PB
PM				ZE	ZE	ZE				ZE	ZE	ZE				ZE	ZE	ZE			
				ZE	ZE	PS				ZE	ZE	PM				ZE	ZE	PB			
PB	ZE	ZE	ZE				ZE	ZE	ZE				ZE	ZE	ZE				PS	ZE	ZE
	ZE	ZE	PS				ZE	ZE	PM				ZE	ZE	PB				PS	PS	PB

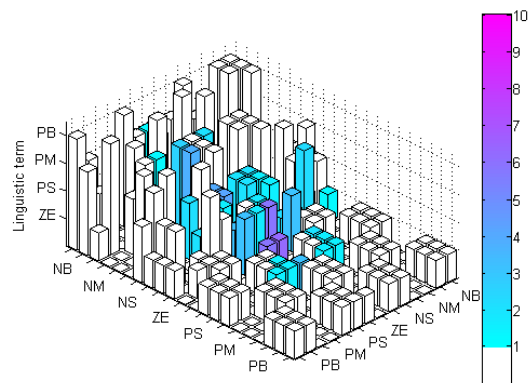
(b)

Fig. 13. The 4 input 2 output control rule-bases (a) Atracurium output rule-base (b)

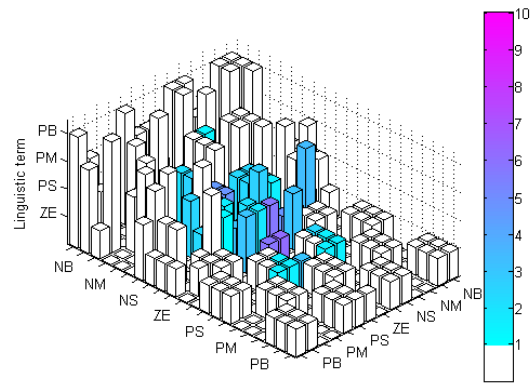
Isoflurane output rule-base



(a)

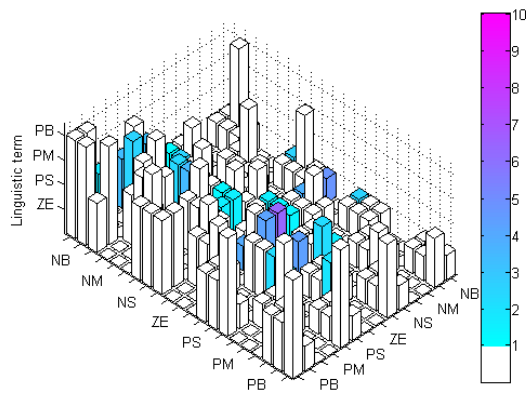


(b)

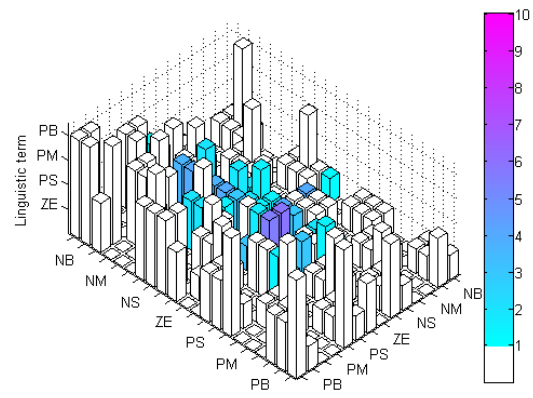


(c)

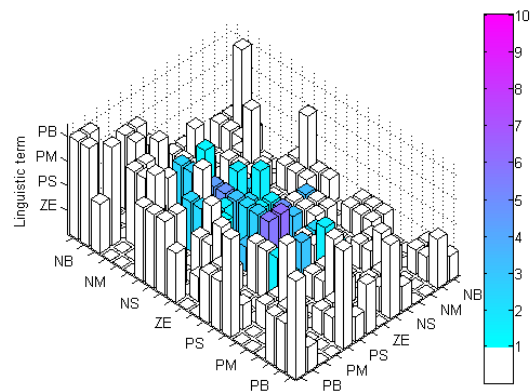
Fig. 14. Firing percentage of Atracurium output rule-base (a) 42-T1-SOFLC (b) 42-IT2_SOFLC (c) 42-GT2-SOFLC



(a)



(b)



(c)

Fig. 15. Firing percentage of Isoflurane output rule-base (a) 42-T1-SOFLC (b) 42-IT2_SOFLC (c) 42-GT2-SOFLC

6. Conclusions

In this paper, we have presented a novel type-2 SOFLC for the automatic control of anesthesia during single stage surgical procedures. The SOFLC is a hierarchical controller which consists of a standard FLC and a SO rule-base mechanism that observes the trajectory of the process to be controlled and corrects any deviations from a desired trajectory path by modifying the FLC's control rule(s). The purpose of our study was to evaluate whether the original type-1 SOFLC could be enhanced by using type-2 fuzzy sets to improve multivariable anesthesia control.

Our type-2 SOFLCs used interval and zSlices based general type-2 fuzzy sets to model variability in the multi variable control parameters, specifically the input parameters for muscle relaxation and BP (used in monitoring DoA) and the output parameters of Atracurium and Isoflurane infusion/concentration rates (used in anesthesia regulation). Clinically acquired data on the average maintained set points for BP (mmHg) and muscle relaxation percentage were collected from 15 anesthetized patients during surgery. The data was used for defining symmetrically shaped FOU's of the Interval and zSlices based general type-2 fuzzy sets using a heuristic approach to capture inter and intra patient parameter variability found in the clinical data, in order to approximate the type-2 FOU's. We used a multivariable non fixed anesthetic model as our patient reference model for conducting surgical simulations which were based on known pharmacological models of the noise added interactions of Atracurium and Isoflurane for regulating muscle relaxation and DoA respectively. The simulations compared the type-2

SOFLCs with type-1 SOFLCs in controlling anesthesia delivery to maintain physiological set points for muscle relaxation and BP over the duration of a single stage operational procedure.

Our results specifically showed that both the interval and zSlices based general type-2 SOFLCs were able to produce a good multivariable control performance in maintaining the desired set points for muscle relaxation and BP in comparison to the type-1 SOFLCs while operating under signal and patient noise. In the case of interval type-2 SOFLC these results concur with experimental evidence that suggests that an interval type-2 FLC will give a smoother control surface in regions around the steady state over its type-1 counterpart [60, 61]. Karnik and Mendel also suggest that interval type-2 FLCs are more adaptive as they are able to realize more complex input-output relationships which cannot be achieved by a type-1 FLC [62]. Our results also support this from the IT2 SOFLCs ability to adaptively regulate multi variable anesthesia set points based on adjusting the delivery rates of two different drugs with different pharmacodynamic and pharmacokinetic characteristics. zSlices based general type-2 fuzzy sets slice the third dimension of a general type-2 fuzzy set into a finite number of interval type-2 fuzzy sets each with a specific height that represents the secondary membership or amplitude associated with all the primary memberships over its FOU [24]. The three dimensional MF of a zSlices based general type-2 fuzzy set can therefore provide greater design degrees of freedom over interval type-2 fuzzy sets [24]. The simulation results we obtained for our GT2-SOFLCs were shown to support this by achieving lower steady state errors for multi variable set point control than the equivalent interval type-2 and type-1 SOFLCs.

We also found that both the interval and zSlices based general type-2 SOFLCs are able to use fewer more concentrated rules to reach the set points via tracking their rule usage. In our simulations we didn't use the rules' firing percentage values as additional inputs into our SO mechanism. Further research can use these values to assign a weight to each rule in order to

improve the rule modification process. In addition, a further deployment of this approach for visualizing the rule usage patterns can help the anesthetist study the drug delivery behavior.

This study has provided good evidence on the merits of using our type-2 SOFLC for automated anesthesia. Compared with the previous FREN system described in [13], our SOFLC is a multi-variable controller for controlling both of MAP (as with FREN) and muscle relaxation. FREN was also applied in a postoperative scenario while the SOFLC is for intraoperative drug delivery control. The FNN in [14] is a multi-variable system for controlling MAP and CO in a postoperative scenario. Two separate sub-controllers are used in [14], which is a similar concept as the decomposition of the multi-variable structure used for SOFLC. However a major difference between the FNN and our SOFLC is that the FNN is able to modify the MFs whereas the SOFLC can self-adapt by modifying the fuzzy control rules.

El-Bardini et al. proposed a direct adaptive IT2-FLC in [16] applied to the same scenario as our study. The direct adaptive IT2-FLC uses a predefined rule-base and tunes the centers of the output MFs of fired rules in response to deviations from the desired control behaviour. Inter and intra-variability is added to the parameters of the patient drug interaction model by manually setting these for specific test cases. In our study we added random noise to both patient model and the measured signals for muscle relaxation and BP to exam the robustness of the controller under environmental and patient related uncertainties. In terms of evaluation of performance, square of errors (ISE), integral of time and absolute error (ITAE) and root mean square error (RMSE) are used as criteria for the direct adaptive IT2-FLC. In our simulations, SSE is the most important criterion to evaluate the performance. It can be proved that the RMSE is greater than or equal to the arithmetic mean error that we used to calculate the SSE. However, the difference of these two types of error will be close to zero for steady state control. Therefore we can use the two errors to roughly compare the performance of the two controllers. By comparison we can

find that even the worst case of the 42-IT2-SOFLC and 42-GT2-SOFLC can still produce a lower error than the best case of the direct adaptive IT2-FLC in [16]. Nevertheless, it should be noted that the RMSE measured for direct adaptive IT2-FLC also counted the settling stage, which leads to a larger overall error. Hence, further research will provide a benchmark comparison to evaluate the performance of the two controllers more precisely. More recent research described in [17] uses genetic algorithms to design fuzzy PID controllers to regulate BIS. The parameters of the fuzzy PID controllers are optimized offline and a cost function is defined to evaluate the performance of the fuzzy PID controllers. However, this controlling structure is quite different from our study so it is difficult to directly compare the performance of this system with our approach. Future research could compare this control strategy to the SOFLCs if we change our monitoring of DoA to use BIS instead of BP as is the case in this study.

In our simulations, we have used a fixed amount of initial bolus which is administered to patients to reach rapid anesthesia. The initial bolus is effective in muscle relaxation in the first 15 minutes and settles down towards the set point. The simulation results show that the bolus can let the system stabilize close to the desired set point which can then be regulated through the adaptive SOFLC. In a real clinical setting it is still however difficult for the anesthetists to decide the amount of the bolus to give. Different patients have different physiological response such as height and weight, and the dosage of initial bolus can therefore also vary in terms of its effectiveness on the patient. Anesthetists generally tend to guess the initial bolus and adjust the amount according to the patient's physiological response. Future work will simulate different amount of initial bolus and see how the type-2 system can handle the related uncertainties and adjustment of the bolus amount to be initially administered.

Our controller is mainly proposed for regulating single stage operation procedure instead of multi stage operation procedures. In such scenarios the depth of anesthesia is not always at the

same level during multi-stage surgical procedure in which the set points may change several times during the operation. Hence, in the future, the set point of muscle relaxation and BP will be changed two or three times during a longer multi-stage simulated procedure to evaluate how well the controller (i.e., Type-2 SOFLC) can handle these changes.

Another proposed feature of the SOFLC which has not been investigated as part of this study is the ability to track and analyze the systems rules that fire over the control period. The dynamic patterns of rule firings can indicate some behavior about the effects of drugs and individual patient's responses to them over the course of a surgical procedure. This would be beneficial to the surgical team during the operation as well as to clinical staff managing the patient's postoperative care.

Acknowledgement

This research was supported by the Center for Dynamical Biomarkers and Translational Medicine, National Central University, Taiwan which is sponsored by Ministry of Science and Technology (Grant Number: MOST103-2911-I-008-001). Also, it was supported by National Chung-Shan Institute of Science & Technology in Taiwan (Grant Numbers: CSIST-095-V301 and CSIST-095-V302).

References

- [1] B. Musizza, S. Ribaric, Monitoring the depth of anaesthesia, *Sensors*, 10 (2010) 10896-10935.
- [2] J. Agarwal, G. Puri, P. Mathew, Comparison of closed loop vs. manual administration of propofol using the Bispectral index in cardiac surgery, *Acta anaesthesiologica Scandinavica*, 53 (2009) 390-397.
- [3] S. Locher, K.S. Stadler, T. Boehlen, T. Bouillon, D. Leibundgut, P.M. Schumacher, R. Wymann,

- A.M. Zbinden, A new closed-loop control system for isoflurane using bispectral index outperforms manual control, *Anesthesiology*, 101 (2004) 591-602.
- [4] M.M. Struys, T. De Smet, S. Greenwald, A.R. Absalom, S. Bingé, E.P. Mortier, Performance evaluation of two published closed-loop control systems using bispectral index monitoring: a simulation study, *Anesthesiology*, 100 (2004) 640-647.
- [5] K. Ejaz, J.-S. Yang, Controlling depth of anesthesia using PID tuning: a comparative model-based study, in: *Control Applications, 2004. Proceedings of the 2004 IEEE International Conference on*, IEEE, 2004, pp. 580-585.
- [6] J. Shieh, M. Abbod, C. Hsu, S. Huang, Y. Han, S. Fan, Monitoring and control of anesthesia using multivariable self-organizing fuzzy logic structure, in: *Fuzzy Systems in Bioinformatics and Computational Biology*, Springer, 2009, pp. 273-295.
- [7] F. Doctor, H. Hagra, V. Callaghan, A type-2 fuzzy embedded agent to realise ambient intelligence in ubiquitous computing environments, *Information Sciences*, 171 (2005) 309-334.
- [8] J. Yadav, A. Rani, G. Garg, Intelligent Heart Rate Controller For Cardiac Pacemaker, *International Journal of Computer Applications*, 36 (2011).
- [9] J.J. Hsu, J.I. Wang, A. Lee, D.Y. Li, C.H. Chen, S. Huang, A. Liu, B.K. Yoon, S.K. Kim, T.J. Tsai, Automated Control of Blood Glucose in the OR and Surgical ICU, in: *Annual International Conference of the IEEE EMBS, Minneapolis, Minnesota, USA, 2009*, pp. 1286-1289.
- [10] M.L. Kumar, R. Harikumar, A.K. Vasan, V. Sudhaman, Fuzzy controller for automatic drug infusion in cardiac patients, in: *Proc. of the International MultiConference of Engineers and Computer Scientists (IMECS 2009)*, Citeseer, 2009.
- [11] D.S. Diwase, R.W. Jasutkar, Expert Controller for Estimating Dose of Isoflurane, *International Journal of Advanced Engineering Sciences and Technologies*, 9 (2011) 218-221.
- [12] C. Jiming, C. Kejie, S. Youxian, X. Yang, Continuous drug infusion for diabetes therapy: a closed-loop control system design, *EURASIP Journal on Wireless Communications and Networking*, 2008 (2008).
- [13] T. Chidentree, U. Sermsak, Biological systems drug infusion controller using FREN with sliding bounds, *Biomedical Engineering, IEEE Transactions on*, 53 (2006) 2405-2408.
- [14] M.E. Karar, M.A. El-Brawany, Automated Cardiac Drug Infusion System Using Adaptive Fuzzy Neural Networks Controller, *Biomedical Engineering and Computational Biology*, 3 (2011) 1-11.
- [15] R. John, S. Coupland, Type-2 Fuzzy Logic: Challenges and Misconceptions [Discussion Forum], *Computational Intelligence Magazine, IEEE*, 7 (2012) 48-52.
- [16] M. El-Bardini, A.M. El-Nagar, Direct adaptive interval type-2 fuzzy logic controller for the multivariable anaesthesia system, *Ain Shams Engineering Journal*, 2 (2011) 149-160.
- [17] H. Araujo, B. Xiao, C. Liu, Y. Zhao, H. Lam, Design of Type-1 and Interval Type-2 Fuzzy PID

Control for Anesthesia Using Genetic Algorithms, *Journal of Intelligent Learning Systems and Applications*, 6 (2014) 70.

[18] T. Procyk, E. Mamdani, A linguistic self-organizing process controller, *Automatica*, 15 (1979) 15-30.

[19] D. Mason, J. Ross, N. Edwards, D. Linkens, C. Reilly, Self-learning fuzzy control of atracurium-induced neuromuscular block during surgery, *Medical and Biological Engineering and Computing*, 35 (1997) 498-503.

[20] J. Ross, D. Mason, D. Linkens, N. Edwards, Self-learning fuzzy logic control of neuromuscular block, *British journal of anaesthesia*, 78 (1997) 412-415.

[21] J. Shieh, D.A. Linkens, A. Asbury, A hierarchical system of on-line advisory for monitoring and controlling the depth of anaesthesia using self-organizing fuzzy logic, *Engineering Applications of Artificial Intelligence*, 18 (2005) 307-316.

[22] J.-S. Shieh, L.-W. Chang, T.-C. Yang, C.-C. Liu, An enhanced patient controlled analgesia (EPCA) for the extracorporeal shock wave lithotripsy (ESWL), *Biomedical Engineering: Applications, Basis and Communications*, 19 (2007) 7-17.

[23] J.-S. Shieh, M.F. Abbod, E.D. Krishna, Y.-C. Chou, S.-Z. Fan, The Simulation of Controlling of Anesthesia Using a Novel Multivariable Fuzzy Logic and Self-Organizing Fuzzy Logic Controller, in: M. Hertzog, Z. Kuhn (Eds.) *General Anesthesia Research Developments*, Nova Science Publishers, Inc., 2009.

[24] C. Wagner, H. Hagra, Toward general type-2 fuzzy logic systems based on zSlices, *Fuzzy Systems, IEEE Transactions on*, 18 (2010) 637-660.

[25] C.-T. Chuang, S.-Z. Fan, J.-S. SHIEH, Muscle relaxation controlled by automated administration of cisatracurium, *Biomedical Engineering: Applications, Basis and Communications*, 18 (2006) 284-295.

[26] J.S. Shieh, D.A. Linkens, J.E. Peacock, Hierarchical rule-based and self-organizing fuzzy logic control for depth of anaesthesia, *Systems, Man, and Cybernetics, Part C: Applications and Reviews, IEEE Transactions on*, 29 (1999) 98-109.

[27] J.-Y. Lan, M.F. Abbod, R.-G. Yeh, S.-Z. Fan, J.-S. Shieh, Review: intelligent modeling and control in anesthesia, *Journal of Medical and Biological Engineering*, 32 (2012) 293-307.

[28] J.-S. Shieh, L.-W. Chang, S.-Z. Fan, C.-C. Liu, H.-P. Huang, Automatic control of anaesthesia using hierarchical structure, *Biomedical Engineering-Applications, basis, communications*, 10 (1998) 195-202.

[29] M.M. Struys, T. De Smet, L.F. Versichelen, S. Van de Velde, R. Van den Broecke, E.P. Mortier, Comparison of closed-loop controlled administration of propofol using Bispectral Index as the controlled variable versus "standard practice" controlled administration, *Anesthesiology*, 95

(2001) 6-17.

- [30] M. Jeanne, C. Clément, J. De Jonckheere, R. Logier, B. Tavernier, Variations of the analgesia nociception index during general anaesthesia for laparoscopic abdominal surgery, *Journal of clinical monitoring and computing*, 26 (2012) 289-294.
- [31] M. Gruenewald, C. Ilies, Monitoring the nociception–anti-nociception balance, *Best Practice & Research Clinical Anaesthesiology*, 27 (2013) 235-247.
- [32] J.-S. Shieh, S.-Z. Fan, L.-W. Chang, C.-C. Liu, Hierarchical rule-based monitoring and fuzzy logic control for neuromuscular block, *Journal of Clinical Monitoring and Computing*, 16 (2000) 583-592.
- [33] O. Meretoja, T. Taivainen, B.W. Brandom, K. Wirtavuori, Frequency of train-of-four stimulation influences neuromuscular response, *British journal of anaesthesia*, 72 (1994) 686-687.
- [34] M. Mahfouf, D. Linkens, A. Asbury, W. Gray, J. Peacock, Generalised predictive control (GPC) in the operating theatre, in: *IEE Proceedings D (Control Theory and Applications)*, IET, 1992, pp. 404-420.
- [35] M. Mahfouf, M. Abbod, A comparative study of generalized predictive control (gpc) and intelligent self-organizing fuzzy logic control (soflc) for multivariable anaesthesia, *Intelligent Control in Biomedicine*, (1994) 79-132.
- [36] L.B. Sheiner, D.R. Stanski, S. Vozech, R.D. Miller, J. Ham, Simultaneous modeling of pharmacokinetics and pharmacodynamics: application to d-tubocurarine, *Clinical pharmacology and therapeutics*, 25 (1979) 358-371.
- [37] B. Weatherley, S. Williams, E. Neill, Pharmacokinetics, pharmacodynamics and dose-response relationships of atracurium administered iv, *British Journal of Anaesthesia*, 55 (1983) 39S.
- [38] B. Whiting, A. Kelman, The modelling of drug response, *Clin. Sci*, 59 (1980) 311-315.
- [39] R. Millard, C. Monk, T. Woodcock, C.P. Roberts, Controlled hypotension during ent surgery using self-tuners, *Computational Biology and Medicine*, 17 (1988) 1-18.
- [40] D. Mason, N. Edwards, D. Linkens, C. Reilly, Performance assessment of a fuzzy controller for atracurium-induced neuromuscular block, *British journal of anaesthesia*, 76 (1996) 396-400.
- [41] M. Mahfouf, D.A. Linkens, *Generalised predictive control and bioengineering*, CRC press, 1998.
- [42] Z. Wu, N.E. Huang, Ensemble empirical mode decomposition: a noise-assisted data analysis method, *Advances in Adaptive Data Analysis*, 1 (2009) 1-41.
- [43] Q. Liang, N.N. Karnik, J.M. Mendel, Connection admission control in ATM networks using survey-based type-2 fuzzy logic systems, *Systems, Man, and Cybernetics, Part C: Applications*

and Reviews, IEEE Transactions on, 30 (2000) 329-339.

[44] X. Du, H. Ying, Derivation and analysis of the analytical structures of the interval type-2 fuzzy-PI and PD controllers, Fuzzy Systems, IEEE Transactions on, 18 (2010) 802-814.

[45] M. Nie, W.W. Tan, Derivation of the analytical structure of symmetrical IT2 fuzzy PD and PI controllers, in: Fuzzy Systems (FUZZ), 2010 IEEE International Conference on, IEEE, 2010, pp. 1-8.

[46] C.W.H. HAgras, Novel methods for the design of general type-2 fuzzy sets based on device characteristics and linguistic labels surveys, (2009).

[47] H. HAgras, F. Doctor, V. Callaghan, A. Lopez, An incremental adaptive life long learning approach for type-2 fuzzy embedded agents in ambient intelligent environments, Fuzzy Systems, IEEE Transactions on, 15 (2007) 41-55.

[48] J.M. Mendel, R.B. John, Type-2 fuzzy sets made simple, Fuzzy Systems, IEEE Transactions on, 10 (2002) 117-127.

[49] J.M. (Eds.), Uncertain Rule-Based Fuzzy Logic Systems: Introduction and New Directions, Prentice Hall, Upper Saddle River, New Jersey, 2001.

[50] H. HAgras, C. Wagner, Towards the wide spread use of type-2 fuzzy logic systems in real world applications, Computational Intelligence Magazine, IEEE, 7 (2012) 14-24.

[51] M.M. Gupta, J.B. Kiszka, G. Trojan, Multivariable structure of fuzzy control systems, Systems, Man and Cybernetics, IEEE Transactions on, 16 (1986) 638-656.

[52] Q. Liang, J.M. Mendel, Interval type-2 fuzzy logic systems: theory and design, Fuzzy Systems, IEEE Transactions on, 8 (2000) 535-550.

[53] D. Wu, M. Nie, Comparison and practical implementation of type-reduction algorithms for type-2 fuzzy sets and systems, in: Fuzzy Systems (FUZZ), 2011 IEEE International Conference on, IEEE, 2011, pp. 2131-2138.

[54] N.N. Karnik, J.M. Mendel, Centroid of a type-2 fuzzy set, Information Sciences, 132 (2001) 195-220.

[55] Y.-C. Chou, M.F. Abbod, J.-S. Shieh, C.-Y. Hsu, Multivariable Fuzzy Logic/Self-organizing for Anesthesia Control, Journal of Medical and Biological Engineering, 30 (2010) 297-306.

[56] D.A. Linkens, S. Hasnain, Self-organising fuzzy logic control and application to muscle relaxant anaesthesia, in: Control Theory and Applications, IEE Proceedings D, IET, 1991, pp. 274-284.

[57] C.T. Hartrick, Y.-S. Tang, D. Siwek, R. Murray, D. Hunstad, G. Smith, The effect of initial local anesthetic dose with continuous interscalene analgesia on postoperative pain and diaphragmatic function in patients undergoing arthroscopic shoulder surgery: a double-blind, randomized controlled trial, BMC anesthesiology, 12 (2012) 6.

[58] J.B. Kruskal, Multidimensional scaling by optimizing goodness of fit to a nonmetric

hypothesis, *Psychometrika*, 29 (1964) 1-27.

[59] F. Wilcoxon, Individual comparisons by ranking methods, *Biometrics bulletin*, 1 (1945) 80-83.

[60] E.A. Jammeh, M. Fleury, C. Wagner, H. Hagrass, M. Ghanbari, Interval type-2 fuzzy logic congestion control for video streaming across IP networks, *Fuzzy Systems, IEEE Transactions on*, 17 (2009) 1123-1142.

[61] D. Wu, W.W. Tan, A type-2 fuzzy logic controller for the liquid-level process, in: *Fuzzy Systems, 2004. Proceedings. 2004 IEEE International Conference on*, IEEE, 2004, pp. 953-958.

[62] N.N. Karnik, J.M. Mendel, Q. Liang, Type-2 fuzzy logic systems, *Fuzzy Systems, IEEE Transactions on*, 7 (1999) 643-658.

Accepted Manuscript

Table 1. Clinical data from 15 anesthetized patients while undergoing a specific Ear, Nose, and Throat (ENT) surgical procedures showing *avg*, *stdv* and calculated *cv* values for Muscle relaxation and BP for each patient and average values for all patients

Patient	Muscle relaxation avg_{mr} , $stdv_{mr}$	CV_{mr}	Blood Pressure (mmHg) avg_{bp} , $stdv_{bp}$	CV_{bp}
1	90.22 (\pm) 9.83	\pm 10.90	84.60 (\pm) 5.66	\pm 6.69
2	89.33 (\pm) 12.43	\pm 13.91	74.96 (\pm) 6.72	\pm 8.96
3	89.38 (\pm) 6.96	\pm 7.79	113.03 (\pm) 12.91	\pm 11.42
4	91.04 (\pm) 9.97	\pm 10.95	89.02 (\pm) 11.95	\pm 13.42
5	89.05 (\pm) 10.43	\pm 11.71	86.05 (\pm) 13.36	\pm 15.53
6	90.82 (\pm) 11.99	\pm 13.20	90.44 (\pm) 16.45	\pm 18.19
7	91.65 (\pm) 11.68	\pm 12.74	92.29 (\pm) 10.69	\pm 11.58
8	90.85 (\pm) 12.82	\pm 14.11	98.21 (\pm) 17.71	\pm 18.03
9	89.04 (\pm) 7.47	\pm 8.39	90.81 (\pm) 23.23	\pm 25.58
10	87.33 (\pm) 10.34	\pm 11.84	90.33 (\pm) 10.31	\pm 11.41
11	86.63 (\pm) 18.09	\pm 20.88	88.48 (\pm) 12.05	\pm 13.62
12	91.41 (\pm) 7.40	\pm 8.10	96.04 (\pm) 7.43	\pm 7.74
13	89.03 (\pm) 9.32	\pm 10.47	93.05 (\pm) 10.64	\pm 11.43
14	89.10 (\pm) 15.68	\pm 17.60	89.60 (\pm) 9.26	\pm 10.33
15	90.46 (\pm) 9.78	\pm 10.81	86.34 (\pm) 17.69	\pm 20.49
Average	89.69 (\pm) 10.95	\pm 12.21	90.88 (\pm) 12.40	\pm 13.64

Notes:

Coefficient of variation (CV) is the ratio of standard deviation to average noise for muscle relaxation and BP respectively.

Table 2. Comparison of 2-input 2-output, 4-input 2-output type-1, interval and general SOFLCs on noise free environment

Type	Inputs	Bolus	SSE_M (normalized units)	SSE_P (mm Hg)	OS_M (%)	US_P (%)	RT_M (min)	DT_P (min)
1	2	NO	0.0846	1.2500	0.8333	0.2391	52.9	1.2
Interval	2	NO	0.0197	0.6434	13.2874	14.9182	4.2	0.6
General	2	NO	0.0321	0.2148	15.5844	16.6582	5.3	0.6
1	2	YES	0.0729	1.2500	23.8453	0.5295	2.1	2.1
Interval	2	YES	0.0068	0.0626	13.5279	0.1286	2.3	3.5
General	2	YES	0.0041	0.0193	13.1408	0.2947	2.3	3.2
1	4	NO	0.0131	0.0652	0.8833	0	61.9	5.1
Interval	4	NO	0.0093	0.2037	0.0867	9.9941	8.9	1.0
General	4	NO	0.0076	0.2563	3.4040	9.9427	8.9	1.0
1	4	YES	0.1534	0.0652	39.2664	0.0449	1.8	4.1
Interval	4	YES	0.0119	0.1029	14.2719	0.0054	2.3	4.1
General	4	YES	0.0022	0.0609	12.8698	0.1360	2.3	3.7

Notes:

1. M represents the value of muscle relaxation and P represents the value of blood pressure.
2. Steady state error (SSE) is the absolute error between the set point value and last average 50 minutes values (for muscle relaxation and BP respectively).
3. Overshoot (OS) is percentage of error between maximum value and average of steady state values.
4. Undershoot (US) is percentage of error between minimum value and average of steady state values.
5. Rising time (RT) is the time taken to rise from 10 percent to 90 percent of the steady state value.

6. Decreasing time (DT) is the time taken to decrease from 10 percent to 90 percent of the steady state values.

Accepted Manuscript

Table 3. Comparison of 4-input 2-output type-1, interval and general SOFLCs on different noise environment

Type	Signal noise	Model noise	SSE_M (normalized units)	SSE_P (mm Hg)	OS_M (%)	US_P (%)	RT_M (min)	DT_P (min)
General	20%	1%	0.0006 (±) 0.0018	0.1353 (±) 0.0446 ^e	13.9251 (±) 0.3040	0.7895 (±) 0.1371	2.3 (±) 0	4.1 (±) 0.9 ^e
	0%	1%	0.0019 (±) 0.0010 ^b	0.0518 (±) 0.0239 ^e	14.2434 (±) 0.2654	0.5784 (±) 0.0694	2.3 (±) 0	3.4 (±) 0.1
	0%	0.75%	0.0019 (±) 0.0009	0.0561 (±) 0.0143	14.0436 (±) 0.2478 ^b	0.4848 (±) 0.0456	2.3 (±) 0	3.5 (±) 0.1
	0%	0.50%	0.0024 (±) 0.0007 ^b	0.0441 (±) 0.0045	13.6932 (±) 0.2196	0.3896 (±) 0.0216	2.3 (±) 0	3.5 (±) 0.1
	0%	0.25%	0.0030 (±) 0.0006	0.0291 (±) 0.0044	13.2503 (±) 0.0957 ^b	0.3094 (±) 0.0188	2.3 (±) 0	3.5 (±) 0
	20%	0	0.0005 (±) 0.0022	0.1133 (±) 0.0450 ^e	12.6545 (±) 0.3520	0.6248 (±) 0.6517 ^e	2.3 (±) 0	4.6 (±) 1.5
	15%	0	0.0019 (±) 0.0023 ^e	0.0599 (±) 0.0244	12.7144 (±) 0.3403	0.2629 (±) 0.0612	2.3 (±) 0	5.8 (±) 2.6
	10%	0	0.0020 (±) 0.0016	0.0355 (±) 0.0277	12.7327 (±) 0.1975	0.1466 (±) 0.0878	2.3 (±) 0	3.8 (±) 0.2
	5%	0	0.0019 (±) 0.0013 ^b	0.0249 (±) 0.0280	12.9493 (±) 0.2261	0.1379 (±) 0.0879 ^e	2.3 (±) 0	3.7 (±) 0.2
	20%	1%	0.0015 (±) 0.0010	0.1441 (±) 0.0138	14.4627 (±) 0.5319	0.5609 (±) 0.1619	2.3 (±) 0.1	4.0 (±) 1.1
	0%	1%	0.0046 (±) 0.0001	0.0683 (±) 0.0005	14.8183 (±) 0.2539	0.5514 (±) 0.0419	2.3 (±) 0.1	2.9 (±) 0.2
	Interval	0%	0.75%	0.0046 (±) 0.0013	0.0808 (±) 0.0160	14.5536 (±) 0.3903	0.4769 (±) 0.0424	2.3 (±) 0.1
0%		0.50%	0.0049 (±) 0.0010	0.0768 (±) 0.0044	14.2618 (±) 0.3213	0.3733 (±) 0.0248	2.3 (±) 0	3.1 (±) 0.1
0%		0.25%	0.0046 (±) 0.0002	0.0694 (±) 0.0013	13.6412 (±) 0.1674	0.3318 (±) 0.0215	2.3 (±) 0	3.1 (±) 0
20%		0	0.0024 (±) 0.0015	0.1432 (±) 0.0205	12.8903 (±) 0.3362 ^a	0.2415 (±) 0.0798	2.3 (±) 0	3.8 (±) 1.9
15%		0	0.0029 (±) 0.0007	0.1200 (±) 0.0067	12.9882 (±) 0.1634	0.1555 (±) 0.0721	2.3 (±) 0	3.5 (±) 1.1
10%		0	0.0034 (±) 0.0008	0.1009 (±) 0.0074	13.0617 (±) 0.0848	0.0719 (±) 0.0466	2.3 (±) 0	3.3 (±) 0.1
5%		0	0.0042 (±) 0.0002 ^a	0.0786 (±) 0.0026	13.2398 (±) 0.2220	0.1334 (±) 0.1031	2.3 (±) 0	3.8 (±) 1.3
20%		1%	0.0066 (±) 0.0036	1.5268 (±) 0.9066	14.1795 (±) 0.7445 ^d	1.8775 (±) 0.8220	2.2 (±) 0.1 ^d	2.2 (±) 0.9
0%		1%	0.0015 (±) 0.0003	0.3193 (±) 0.0045	14.1267 (±) 0.4629 ^d	0.4902 (±) 0.0660	2.3 (±) 0.1 ^d	3.9 (±) 0.2
0%		0.75%	0.0015 (±) 0.0009	0.3696 (±) 0.0397	13.9437 (±) 0.3380	0.3350 (±) 0.0324	2.3 (±) 0.1 ^d	4.0 (±) 0.2
0%		0.50%	0.0019 (±) 0.0012	0.3522 (±) 0.0432	13.3786 (±) 0.3089	0.2909 (±) 0.0691	2.3 (±) 0.1 ^d	4.0 (±) 0.1
1		0%	0.25%	0.0014 (±) 0.0008	0.3319 (±) 0.0245	13.1295 (±) 0.1541	0.1851 (±) 0.0534	2.3 (±) 0.1 ^d
	20%	0	0.0061 (±) 0.0031	1.9258 (±) 0.7372	13.3511 (±) 0.8646	1.7413 (±) 0.6235	2.3 (±) 0 ^d	2.4 (±) 0.7 ^d
	15%	0	0.0068 (±) 0.0028	1.9984 (±) 0.7626	13.4445 (±) 0.7136 ^d	1.3248 (±) 0.9132	2.3 (±) 0 ^d	2.7 (±) 0.9 ^d
	10%	0	0.0085 (±) 0.0058	1.6441 (±) 1.0900	13.4762 (±) 0.7346	1.1958 (±) 0.7975	2.3 (±) 0 ^d	2.7 (±) 0.8
	5%	0	0.0148 (±) 0.0212	1.4795 (±) 0.8809	13.8477 (±) 0.9284 ^d	1.2743 (±) 0.8032	2.3 (±) 0 ^d	2.5 (±) 0.9 ^d

^a Reject hypothesis: 42-T1-SOFLC produces different SSE compared with 42-IT2-SOFLC.

^b Reject hypothesis: 42-T1-SOFLC produces different SSE compared with 42-GT2-SOFLC.

- ^c Reject hypothesis: 42-GT2-SOFLC produces different SSE compared with 42-IT2-SOFLC.
- ^d Reject hypothesis: There is significant difference among the three 4 input 2 output SOFLCs.

Accepted Manuscript

Type-2 Fuzzy Sets Applied to Multivariable Self-Organizing Fuzzy Logic Controllers for Regulating Anesthesia

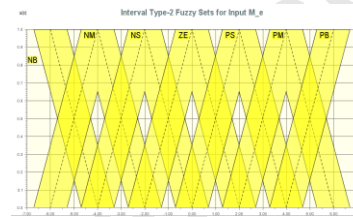
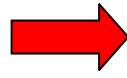
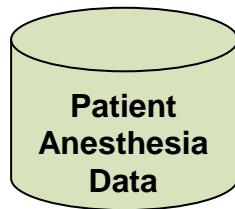
Faiyaz Doctor¹ Chih-Hao Syue² Yan-Xin Liu² Jiann-Shing Shieh² Rahat Iqbal¹

¹Department of Computing, Coventry University, Coventry, CV1 5FB, United Kingdom

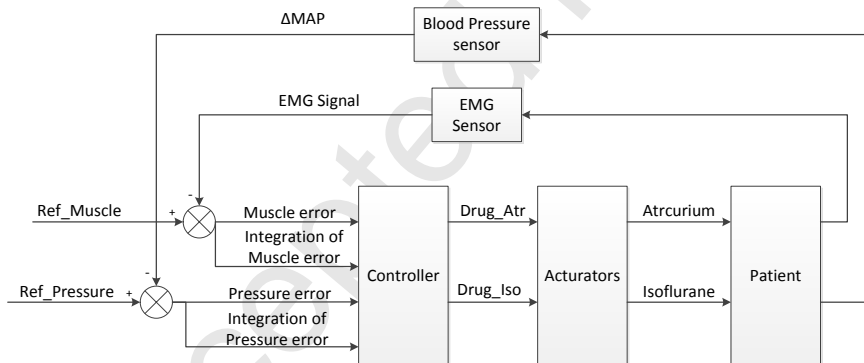
²Department of Mechanical Engineering, and Innovation Center for Big Data and Digital Convergence, Yuan Ze University, Chungli, 320, Taiwan, ROC

Email: faiyaz.doctor@coventry.ac.uk

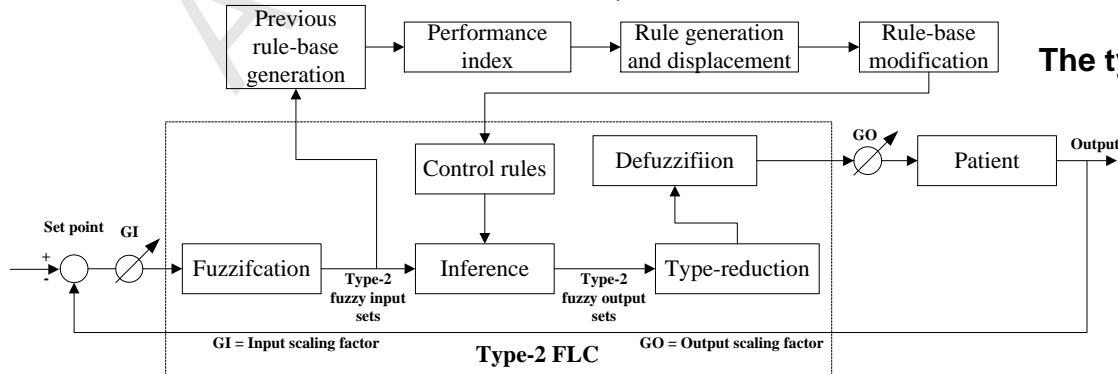
Graphical Abstract for Review



Type-2 fuzzy sets representing patient and operational uncertainties in physiological input signals / output drug delivery rates



The multivariable anesthesia system with signal and model noise emulating patient related and surgical uncertainties



The type-2 SOFLC